Natural Hazards (2024) 120:6797–6832
https://doi.org/10.1007/s11069-024-06491-7

ORIGINAL PAPER

Landslide susceptibility mapping using morphological and hydrological parameters in Sikkim Himalaya: frequency ratio model and geospatial technologies

Irjesh Sonker[1] · Jayant Nath Tripathi[1] · Swarnim[1]

Received: 31 January 2024 / Accepted: 1 February 2024 / Published online: 4 March 2024

Abstract
Sikkim Himalaya, a part of the North-Eastern Himalayan region, is affected by the landslides and it causes the loss of life, property, and other human infrastructure, etc. The objective of study is identification of landslides susceptibility zones of the Sikkim Himalaya, using various factors/thematic layers, such as absolute relief, relative relief, relief ratio, dissection index, hypsometric integral, slope index, drainage density, drainage frequency, drainage intensity, drainage texture, infiltration number, junction frequency, length of overland flow, ruggedness index, stream transport index, topographic wetness index, stream power index, and rainfall and all these layers are integrated in Arc GIS software using FR model. These spatial factors are generated using Alos Palsar DEM and rainfall data with the help of the Arc GIS. The FR model was utilised for the purpose of determining the weights of such all-thematic layers for the possibility of landslides occurring in regions that are susceptible to the effects of landslides. These weight of such all thematic layers are combined using the Arc GIS to create the map of landslide susceptibility zones. The map of the landslide susceptibility zones of the region has been split into five distinct categories, including 'very high' (13.20%), 'high' (19.75%), 'moderate' (30.81%), 'low' (27.14%), 'very low' (9.09%). For accuracy analysis of the model the area under the curve is used and is estimated as 84.6% with the help of the FR model and occurrence of previous landslides in the region.

Keywords Morphometrical · Hydrological · Remote sensing and GIS · Frequency ratio model · Sikkim Himalaya

1 Introduction

Natural disasters such as earthquakes, avalanches, landslides, and glacier lake outburst flood (GLOFs) represent a major threat to life and infrastructure damage in Himalayan terrain mainly (Chowdhuri et al. 2022a). Landslides have recently occurred in India's

✉ Jayant Nath Tripathi
jntripathi@gmail.com

[1] Department of Earth and Planetary Sciences, University of Allahabad, Prayagraj 211002, India

Himalayan hilly regions, causing destruction of infrastructure and cultural heritage (CH), loss of life, traffic challenges ranging from mildly inconvenient to catastrophic, and it impact on the economy's foundation (Kumar et al. 2018; Saha et al. 2021; Chakrabortty et al. 2022; Sonker et al. 2022). Because of intense tectonic movement, the Himalayan have terrain that is steep and a complex geological structure that causes avalanches, mass movements, and earthquakes. Among the many mountainous hazards that occur in the Himalayan region, landslides happen to be the most frequent and prominent occurrences. Overall, 80% of all landslides happen in India's Himalayan area, and particularly during the period with the most precipitation, the "Gharwal Himalaya, Himachal Himalaya, Kumaun Himalaya, Sikkim-Darjeeling, and middle Himalaya" have all seen several disastrous landslide incidents (Chowdhuri et al. 2022b; Islam et al. 2022).

In India, the Sikkim Himalaya of North-East Himalayan is one of the most susceptible regions for the landslide occurrence. This is because of transforming a forest area into cleared land, heavy rainfall, constructing more human settlement and industrialization, and changes in climate have all caused landslides here at all spatial scale (Bhattacharya 2013; Skilodimou et al. 2018; Tripathi et al. 2022). All of which have resulted in greater rock degradation and waterlogging of the soil that generates landslides on gentle to sharp and scraping gradients in the hilly terrain (Bhattacharya 2012, 2013; Chamling 2013; Mandal and Maiti 2013). Each year, hundreds of human lives are lost by landslides in the Sikkim Himalaya. More than 36,000 people have been killed in the year of 1968 due to the landslide (Bhasin et al. 2002; Kaur et al. 2019).

Therefore, the use of landslide susceptibility zonation (LSZ) is considered the initial stage in landslide risk zones preparation, analysis, and elimination. Due to this, numerous authors over the world have utilised these stages for identification of landslide susceptibility zonation (Gupta and Joshi 1990; Van Westen 1994; Binaghi et al. 1998; Gupta 2003; Sarkar et al. 2006; Lee 2005; Nefeslioglu et al. 2008, 2010; Pradhan et al. 2010; Pourghasemi et al. 2012a, b; Kayastha et al. 2013; Dou et al. 2015; Sangchini et al. 2016; Pal and Chowdhuri 2019; Basu and Pal 2020; Sonker et al. 2021, 2022). In recently, landslide susceptibility zonation (LSZ) map is a map that utilizes remotely sensed data and geographic information systems (GSI) to identify areas that are susceptible to landslides which produce better high precision outcomes. To make a landslide susceptibility zonation (LSZ) map, it is now necessary to make a factor/thematic layer of landslide causes and give each of them a calculated weight. Remote sensing is a useful tool because it works in space and time, as well as repeatedly collecting data, and it can also be used in inaccessible locations (Yalcin et al. 2011; Anbalagan et al. 2015; Zhao and Lu 2018; Mersha and Meten 2020; Gupta et al. 2022; Taloor et al. 2021a, b, c; 2022). Through the utilisation of GIS, we may collect geospatial data gathered from remote sensing and several different data products for use in assessment, modelling, simulations, and visual analytics, all of which help us arrive at more informed conclusions (Ilanloo 2011; Kannaujiya et al. 2019; Velayudham et al. 2021; Islam et al. 2022).

In this study, we utilise a frequency ratio (FR) method in remote sensing (RS) and a geographic information system (GIS) setting to determine potential landslide susceptibility zones by analysing a variety of morphometric and hydrological features. Morphometry is a term that is widely used to refer to the process of quantifying and performing statistical modelling on the arrangement of the surface of the earth, as well as the shape and size of the earth's landforms (Horton 1945; Miller 1953; Melton 1957; Clarke 1996; Agarwal 1998; Reddy et al. 2002; Yangchan et al. 2015; Farhan 2017; Bhatt et al. 2020; Sonker et al. 2023). The study of morphometric parameters measures the condition of the geo-hydrological phenomenon of a drainage basin of the study region, which also represents

the predominant climate condition, lithology types, landforms, and other characteristics of the region (Horton 1932, 1945; Strahler 1952; Mueller 1968; Cox 1994; Oguchi 1997; Mishra and Rai 2020). Hydrological parameters represent sediment transportation during surface runoff and the region's moisture condition, which help understanding of the surface condition of the drainage basin (Rekha et al. 2011; Sreedevi et al.2013; Soni 2013). The goal of the research is to learn how the combination of morphometry and hydrological parameters can help us understand landslide susceptibility zonation mapping.

Researchers have used morphometric parameters to learn more about areas of the Himalayas that are prone to landslides (Ghosh 2015; Das and Lepcha et al., 2019). Therefore, the researcher has used morphometric parameters such as drainage density, drainage frequency, junction frequency, relative relief, relief ratio, altitude, texture, slope, and other responsible factors for landslides to generate the landslide susceptibility zonation map (Devkota et al. 2013; Anbalagan et al. 2015; Ghosh 2015; Rawat et al. 2017; Das and Lepcha et al. 2019; Saha et al. 2022). The hydrological parameters TWI (topographic witness index), SPI (stream power index), STI (stream transportation index), and rainfall have also been used by several researchers to generate the LSZ map (Rożycka et al. 2017; Kalantar et al. 2018; Das and Lepcha et al. 2019; Moazzam et al. 2020, Sur et al. 2020; Sonker et al. 2022). The major causes of landslide in the Sikkim Himalaya are the rainfall in rainy season, so this factor plays major role for help to understand the morphometric and hydrological analysis for the LSZ mapping in this region.

The objectives of this study are: (1) the integration of the morphometric and hydrological parameters for the mapping of the landslide susceptibility zonation with the help of remote sensing data and GIS, (2) this map of landslide susceptibility zonation is validated and calculated with accuracy using the landslide inventory location for predicting the possibility of landslide susceptibility in interior regions of the state of Sikkim.

2 Materials and methods

2.1 Study area

The Sikkim Himalaya (Fig. 1) lies mostly in the Lesser and Greater Himalaya of the North-Eastern Himalayan, and is made up of a younger mountain structure with faulting and folding. The topography of the region is entirely hilly, with less flat areas, and the elevation varies from 240 to above 8000 m, above mean sea level (msl). The area's latitude and longitude are 27° 5′ to 28° 10′ and 88° 01′ to 88° 58′. The length of the state from north to south is 113 kms, while the width of the region from east to west is 65 kms. The total land area of the region is 7096 square kilometres. Nepal, Bhutan, Tibet, the state of West Bengal surrounds it on the west, east, north, and south, respectively. The state of Sikkim has four districts: North, East, South, and West Sikkim. Sikkim's largest district is North Sikkim, which has a land area of 4226 km^2 and contributes for almost 60% of the surface area of the state. The remaining three districts have included East, West, and South Sikkim, each of which covers around 13%, 16%, and 11% of the total surface area, respectively. Gangtok, the state capital and most important city, is located in North Sikkim district. The region contains two rivers such as the Teesta River and Rangit River. The landforms and river systems of the Teesta River are primarily distinguished by the presence of four-tiered terraces, canyons or gorge-valleys at various elevations, asymmetric valleys, polyprofilic U-shaped valleys and steps or

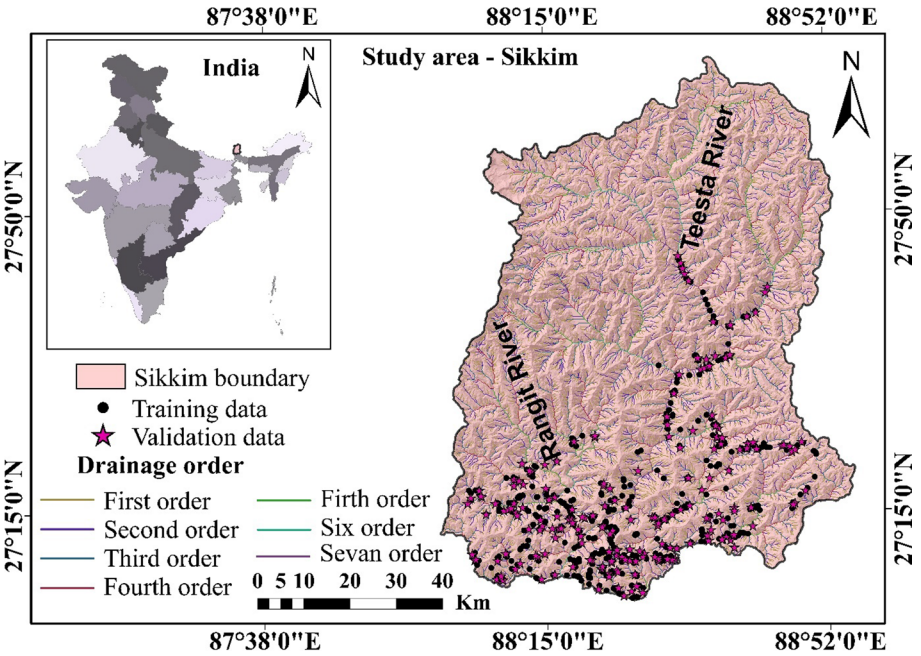

Fig. 1 Study map of the Sikkim Himalaya with location of the landslide inventory and drainage order of the region

troughs, lakes, alluvial cones, truncated ridge-spurs, and terracettes (soil landscape systems). The river exhibits many different types of river systems, ranging from straight to meandering and braided channels, including rectangular-barbed-parallel-trellis-radial to sub dendritic river systems. Each of the above physical characteristics shows that degradation, erosion, and deposition are still happening in the region, which makes it very fragile. The climate of the area can be generally classified as tropical, temperate, or alpine zone. Humidity and cold dominate the weather pattern for the majority of season. The majority of the region has consistently high rates of rainfall from May to October.

2.2 Landslide inventory data

The concept of "landslide inventory location" refers to the historical data on landslides that have happened in various locations and at different periods. It is used for the forecasting of the LSZ mapping and evaluations of risk (Wu et al. 2016; Sonker et al. 2021). Landslide's locations for the inventory (Number of landslides are 688 and locations show in Fig. 1) were gathered from the Bhukosh portal (Geological Survey of India) and utilized to assessment and validity of the present research. These inventory locations are separated among two separate categories as random, such as training data, which is utilized 70% (479) to generate the FR model, and validation and result verification, utilizing 30% (209) of the data. The aim of the current inventory was to forecast and minimize the potential of future landslides.

2.3 Steps for identification of landslides susceptibility mapping

The Sikkim Himalaya regions that are susceptible to landslides prone are identified using a frequency ratio and geospatial tools method based on the assessment of morphometric and hydrological parameters. Frequency ratio model is used to analyse the landslide susceptibility map in this area with the help of the Arc GIS tools. In this model, weights of the factors are calculated on the basis of landslide inventory location and factors classes of the morphometry and hydrological parameters. Therefore, each step of the methodology for the LSZ mapping are given below:

2.3.1 Generating thematic layers

The drainage order of the study area was extracted using Alos Palsar (spatial resolution of 12.5 m) DEM (Digital Elevation Model) data and the order is seven which is validated with toposheet of Sikkim (Survey of India) (Because they belong to a border state, not all toposheets are available.). The Alos Palsar-DEM data was downloaded from Earth Data (https://asf.alaska.edu/data-sets/sar-data-sets/alos-palsar/). The drainage system and DEM data of the study area used to generate different raster maps of morphometric parameters (factors of drainages and relief) with the help of different formula given in Table 1 and the class of the factor in Table 2**,** such as absolute relief (Ar), relative relief (R), relief ratio (Rh), dissection index (Di), hypsometric integral (HI), slope index (Sl), drainage density (Dd), drainage frequency (Fs), drainage intensity (Di), drainage texture (Dt), infiltration number (If), junction frequency (Jf), length of overland flow (Lg), ruggedness index (Rn), with the help of the Arc GIS Software, as shown in Fig. 2a–n. The hydrological parameters such as stream transport index (STI), topographic wetness index (TWI), stream power index (SPI), were generated using DEM data with the help of the Arc GIS, as shown in Fig. 2o–q. Rainfall (Rf) map was generated using rainfall data using Arc GIS, as shown in Fig. 2r. Daily rainfall data from 1988 to 2018 was collected by IMD, Pune (Indian Metrological Department, Pune (https://www.imdpune.gov.in/).

2.3.2 The logic that involved into choosing of the different factor/thematic layers

Landslides typically happen owing to a range of variables, such as high precipitation and subsoil wetness, gradient variability, landscape degradation, forest degradation, subsurface composition, etc. in different areas of the study region. The morphometric and hydrological parameters are preferred based on this above condition. Landslide-causing circumstances can be assessed with the use of these variables. Explanation of the logic involved into choosing of such factor/thematic layers are shown in Table 3.

2.3.3 The scale/weight procedure as well as its justification of the factors in FR model

All the thematic layers are classified into 10 classes. The scale/weight has been classified into a 10 ranked scale where 0 is the lowest and 1 is the highest effect of the landslide occurrence with respect to the factors which are selected for landslide phenomenon

Table 1 The process of determining various morphometric (drainage and relief factors) and hydrological parameters

Factors	Formula of the factors	References
Relative relief (Rr)	Rr = H–h, where, H = maximum height of the region, h = minimum height of the region	Schumm,1956
Relief ratio (Rh)	Rh = Rr/Lb, where, Rr = relative relief of the region, Lb = length of the region	Schumm 1956
Dissection index (Di)	Di = Rr/Ar, where, Rr = relative relief, Ar = absolute relief	Deolia & Pande 2014
Hypsometric integral (HI)	$HI = (h_{mean} - h_{min})/(h_{max} - h_{min})$, where, h_{mean} = mean elevation, h_{min} = minimum elevation, h_{max} = maximum elevation	Schumm 1956
Drainage density (Dd)	$Dd = L/A$, where, L = length of drainage, A = area of region	Horton 1945
Drainage frequency (Fs)	$Fs = N/A$, where, L = number of drainages, A = area of region	Horton 1945
Drainage intensity (Di)	DI = Fs/Dd, where, Fs = drainage frequency, Dd = drainage density	Faniran 1968
Drainage texture (Dt)	Dt = N/P, where, N = number of drainages, P = perimeter of the region	Horton 1945
Infiltration number (If)	If = Dd × Fs, where, Fs = drainage frequency, Dd = drainage density	Faniran 1968
Junction frequency	Number of join points of the drainage in each grid of the region	Das & Lepcha 2019
Length of Overland flow (Lg)	Lg = 1/(2Dd), where, Dd = drainage density	Horton 1945
Ruggedness index (Rn)	Rn = Rr × Dd, where, Rr = relief of the region, Dd = drainage density	Schumm 1956
SPI	$SPI = C \times \tan(d)$, where, C = total catchment area (specific unit is m^2/m) and d = slope gradient (degree) in the region	Moore et al. 1991
STI	$STI = (C/(22.13))^{0.6} \times (\sin(d)/(0.0896))^{1.3}$, where, C = total catchment area (specific unit is m^2/m) and d = slope gradient (degree) in the region	Moore et al. 1993
TWI	$TWI = \ln(C/\tan(d))$, where, C = total catchment area (specific unit is m^2/m) and d = slope gradient (degree) in the region	Moore et al. 1991

Table 2 Range values of the classes of various morphometric (drainage and relief factors) and hydrological parameters

Factors	Class
Relief parameters	
Absolute relief (Ar)	> 6000 ≤ 1500 (m)
Relative relief (Rr)	30–2496 (m)
Relief ratio (Rh)	0.0019–0.0221 (m)
Dissection index (Di)	0.02–0.85
Hypsometric integral (HI)	0.18–0.77
Slope index (Sl)	0–84 (Degree)
Drainage parameters	
Drainage density (Dd)	0.71–4.24 (km/sq km)
Drainage frequency (Fs)	0–9.57 (No. of drainage/sq km)
Drainage intensity (DI)	0–4.76
Drainage texture (Dt)	0–2.13 (No. of drainage/km)
Infiltration number (If)	0–37
Junction frequency (Jf)	0–9
Length of overland flow (Lg)	0.35–2.12 (km)
Ruggedness index (Rn)	0.0098–0.9902
Hydrological parameters	
SPI	− 3.15–13.3
STI	0–409.92
TWI	1.11–18.81
Rainfall (Rf)	> 3200 ≤ 2600 (mm)

occurrences. Table 4 below illustrates the weight procedure and the logic for the scale/weight.

2.3.4 Frequency ratio (FR) Model

The Frequency ratio (FR) model is utilized in this study. The FR model is the statistical method that is currently being utilized to evaluate landslide susceptibility zonation (LSZ). This model is used to figure out the relationship between the reported geographical distribution of prior landslides and all of the factors that are considered to be the primary contributors to the occurrence of landslides. Many researchers have utilized this model for LSZ mapping (Yilmaz 2009; Mezughi et al. 2011; Choi et al. 2012; Mohammady et al. 2012; Yalcin et al. 2011; Lee 2014; Anbalagan et al. 2015; Das and Lepcha 2019; Mirdda et al. 2020; Sonker et al. 2022).

The FR method can be utilized for figure out how much that every component has an impact in zonation mapping of landslides. The FR model is calculated (Table 5), given below:

$$\mathrm{FR} = \frac{a/b}{c/d}$$

where frequency of landslides for each factor class (a), sum of all landslides that are present in the factor (b), frequency of pixels of each class of factor having landslides happen (c), and the sum of all number of the pixels that are present in the factor (d).

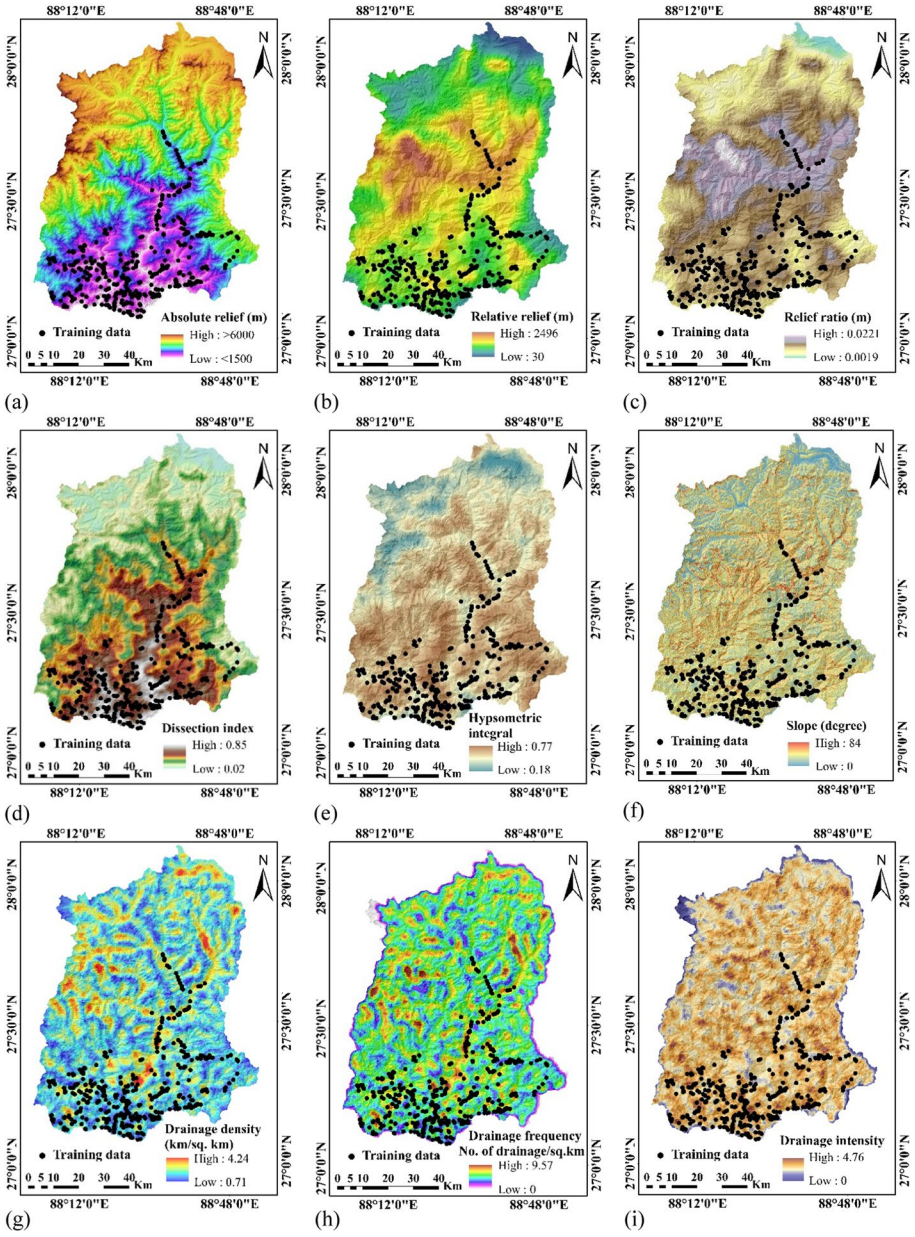

Fig. 2 Factor/thematic layer for different morphological and hydrological parameters: **a** absolute relief, **b** relative relief, **c** relief ratio, **d** dissection index, **e** hypsometric integral, **f** slope index, **g** drainage density, **h** drainage frequency, **i** drainage intensity, **j** drainage texture, **k** infiltration number, **l** junction frequency, **m** length of overland flow, **n** ruggedness index, **o** SPI, **p** STI, **q** TWI, and **r** rainfall for the landslide susceptibility zonation mapping in Sikkim Himalaya

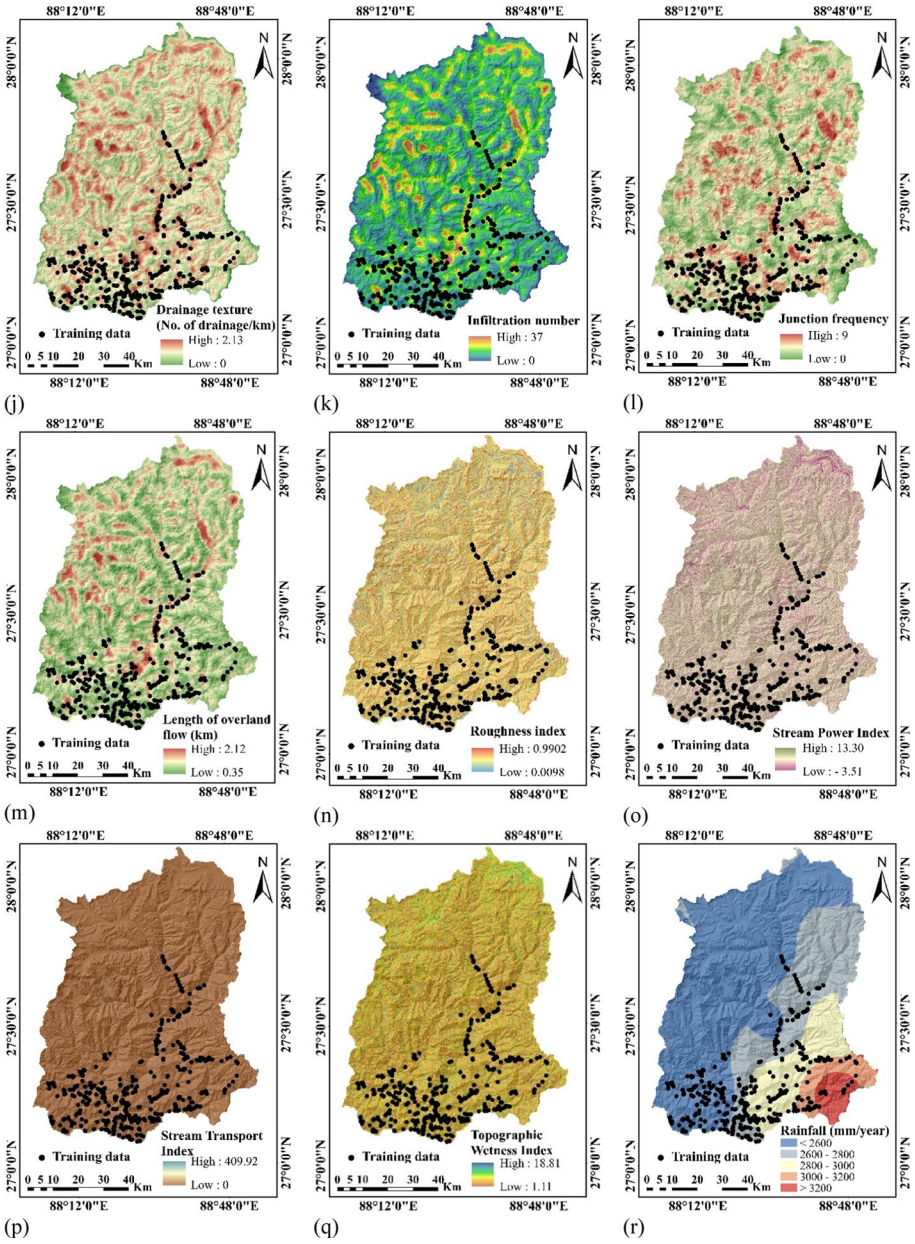

Fig. 2 (continued)

Greater correlations between landslide phenomena and influencing factors are shown by FR values greater than one, whereas lower correlations are indicated by FR values less than one (Fig. 3).

The calculated FR values, it's are normalized and the normalized FR is calculated (Table 5) as given below:

Table 3 The logic for choosing the factors of morphometry and hydrological parameters

Factors	Logic for choosing the factors
Relief parameters	
Absolute relief (Ar)	This factor is the DEM data, which indicates the lowest and highest altitudes of the study area. It generates the gradient of the surface, which influences flow and material movement (Babu et al. 2016; Saha et al. 2022)
Relative relief (Rr)	This factor is a key characteristic of the topography of an area that indicates the effects of erosion or uplift and also indicates the tectonics of the area (Qiu et al. 2018). This component represents the geometrical conditions that promote the formation of landslides
Relief ratio (Rh)	This factor is very important in predicting the durability of the underneath rock and the slope gradient of the area (Mahadevaswamy et al. 2011; Basu and Pal 2019)
Dissection index (Di)	This index alludes to the sloped degradation or separation degree of landscape changes. It demonstrates how, over time, the landscape varies across all geographical and climatic regions
Hypsometric integral (HI)	The hypsometric integral is a useful indicator that correlates strongly with the degree of dissection by the drainage network to determine the specific developmental stage of a landscape. The HI also indicate surface runoff, sediment erosion, and tectonic evolutions of the region (Strahler 1952; Mishra and Rai 2020)
Slope index (Sl)	Trigger for a mass movement could be a change in slope angle. This slope angle can be produced by a variety of causes, including tectonic upliftment, surface erosion caused by various agents, climate change, morphometric index, etc. (Claessens et al. 2013; Donnarumma et al. 2013)
Drainage parameters	
Drainage density (Dd)	This factor is a good way to measure and evaluate the natural landscape, even though it is affected by changes in climate, rock properties, structural features, soil type, and the regionals topography. It can be used as a key marker to show how some of these things happened and how landforms were made (Melton 1957; Sonker et al 2021)
Drainage frequency (Fs)	The amount of rain that falls, how thoroughly it soaks in the area, how quickly it runs off, how porous the ground is, and how steep the slope are all factors that influence the frequency of drainage (Kale and Gupta 2001; Prabhakaran and Jawahar Raj 2018; Adhikari 2020)
Drainage intensity (DI)	A quantity for drainage intensity reveals how much the surface has been dissected by geomorphic agents, and hence how much slower or faster the runoff is being drained from the basin (Strahler 1964; Farhan 2017)
Drainage texture (Dt)	This factor is dependent on the characteristics of the soil, including its type and pattern of vegetation, types of rocks and their composition, the capacity and density of infiltration, as well as the frequency and spacing of drainage, all of which have a direct correlation to drainage textures and the evolution of the landscape (Horton 1945; Smith 1950; Kale and Gupta 2001)
Infiltration number (If)	It reveals the basin's propensity for infiltration and the nature of its discharge. An increase in infiltration can accelerate the growth of a landslide (Strahler 1964; Prabhakaran and Jawahar Raj 2018)
Junction frequency (Jf)	The frequency at which two or more streams converge at a single location is a difference that can be attributed to the instability of slope gradient, since slope failures occur at points where the more than one stream converge
Length overland flow (Lg)	This factor represents the physico-hydrological behaviour of the river basin. It denotes the time it takes for water to travel across land before forming distinct river courses (Horton 1945; Kale and Gupta 2001; Prabhakaran and Jawahar Raj 2018)

Table 3 (continued)

Factors	Logic for choosing the factors
Roughness index (Rn)	This factor is a morphometric measure that depicts the heterogeneity or instability of the terrain; it describes the surface as rugged or smooth terrain, as well as the composition and structure of the landform (Strahler 1956; Nakileza and Nedala 2020)
Hydrological parameters	
SPI	This factor assesses a stream's ability to transport material and is directly related to the occurrence of landslides (Moore 1991; Pawluszek and Borkowski 2017; Sur 2020)
STI	This factor gives details about how earth mass movement and deposition, as well as where they are in space (Moore and Wilson 1992; Ahmad 2019)
TWI	This factor is often utilized to evaluate and analyse how terrain impacts hydrological conditions. High soil moisture causes the soil stability to decline, which makes landslides more likely (Beven and Kirkby 1979; Sörensen 2006; Das and Lepcha 2019; Abu El-Magd et al. 2021)
Rainfall (Rf)	Rainfall is the most significant contributing factor that can cause landslides in regions with moderate to high gradient. Because of its ability to create landslides, it causes soil to get saturated and then runoff, which is caused by water penetrating the soil and leading to increasing pore-water pressure (Long and De Smedt 2018)

$$\mathrm{FRn} = \frac{\mathrm{FR}}{\Sigma \mathrm{ClassFR}}$$

Therefore, the landslide susceptibility index (LSI) map is generated by adding all values of normalised FR with their factor. This is a quantity that has no dimensions and is utilised for the categorization of landslide susceptibility zonation:

$$\mathrm{LSI} = \Sigma\, \mathrm{FR}\neg\mathrm{n}$$

where FRn represents the normalization of FR for each factor class.

There are different ways to categorize the landslide susceptibility index, but in this study, the natural break is used.

3 Result and discussion

3.1 Frequency ratio model for landslide susceptibility mapping

The frequency ratio model was utilised to categorize the susceptibility map into the following five categories: "very high," "high," "moderate," "low," and "very low" (Fig. 4). These categories, when applied to the region as a whole, represent, respectively, 13.20%, 19.75%, 30.81%, 27.14%, and 9.09% of the total area as shown in Fig. 5a. The lower side of the study region, mainly West, South, and East Sikkim, may have higher chances of the occurrence of a landslide with very high to high susceptibility (about 32.95% of the total study area) (Fig. 5a). These regions represent about 86.78% of the total number of prior landslides that are shown in Fig. 5b. It contains the highest density of landslide inventory locations (Fig. 6). The FR model indicates how probable or essential each class is to trigger a landslide based on our variables for multiple classes of each factor. In the case of the

Table 4 The scale/weight process for factors as well as its justification of the factors for morphometry and hydrological parameters

Factor	Scale/weight procedure	Logic for scaling/weight
Relief parameters		
Absolute relief (Ar)	The score of 1 has the highest impact for landslides, and the scores continue to decline until they reach 0, which has the least impact for landslides	Higher elevations are indicative of more recent geologic activity, which indicates the landslide event phenomenon, and vice versa (Rawat 2012; Rawat et al. 2017)
Relative relief (Rr)	The score of 1 has the highest impact for landslides, and the scores continue to decline until they reach 0, which has the least impact for landslides	A low proportion of relative relief indicates that the gradient is either totally flat or merely very gently sloping. Because of this, the volume of surface runoff has decreased, which suggests that the number of landslides has also decreased, and vice versa (Qiu et al. 2018)
Relief ratio (Rh)	The score of 1 has the highest impact for landslides, and the scores continue to decline until they reach 0, which has the least impact for landslides	When the relief ratio is low, it means that the ground below is rigid and that there isn't as much of a gradient, which means that landslides are less likely to happen, and vice versa (Chopra et al. 2005)
Dissection index (Di)	The score of 1 has the highest impact for landslides, and the scores continue to decline until they reach 0, which has the least impact for landslides	If the dissection index is high, then the landscape is unstable and prone to landslides; conversely, if it is low, then the probability of a landslide is lower (Pandey et al. 2018; Ghosh 2015)
Hypsometric integral (HI)	The score of 1 has the highest impact for landslides, and the scores continue to decline until they reach 0, which has the least impact for landslides	High hypsometric integrals indicate an unstable surface that is prone to landslides, and vice versa (Lin et al. 2011; Sonker et al. 2023)
Slope index (Sl)	The score of 1 has the highest impact for landslides, and the scores continue to decline until they reach 0, which has the least impact for landslides	One of the most important aspects that might play a role in the triggering of a landslide is the slope of the terrain. The existence of a considerable quantity of slope is predictive of an enhanced chance of the potential of a landslide being caused by this phenomenon when slope score is higher, and vice versa (Sonker et al. 2021; Mersha and Meten 2020)
Drainage parameters		
Drainage density (Dd)	The score of 1 has the highest impact for landslides, and the scores continue to decline until they reach 0, which has the least impact for landslides	Streams that have a strong drainage density generally exhibit streamflow that have a tendency to be higher runoff and have a high dropping slope area. This is because they have a higher volume of water flowing through them. Therefore, dense drainage systems indicate a greater prone to landslides (Mandal and Mandal 2016)

Table 4 (continued)

Factor	Scale/weight procedure	Logic for scaling/weight
Drainage frequency (Fs)	The score of 1 has the highest impact for landslides, and the scores continue to decline until they reach 0, which has the least impact for landslides	Higher discharge results from higher stream frequency because permeability and infiltration are reduced which indicates high chances of the landslide occurring
Drainage intensity (DI)	The score of 1 has the highest impact for landslides, and the scores continue to decline until they reach 0, which has the least impact for landslides	A lower score for drainage intensity suggests that drainage density and frequency have had a minor influence on the degree to which the landscape has been eroded by the denudation agents (Faniran 1968; Rai et al. 2018)
Drainage texture (Dt)	The score of 1 has the highest impact for landslides, and the scores continue to decline until they reach 0, which has the least impact for landslides	Higher surface run off results from higher drainage texture which indicates higher chances of material erosion and vice versa (Strahler 1964)
Infiltration number (If)	The score of 1 has the highest impact for landslides, and the scores continue to decline until they reach 0, which has the least impact for landslides	The infiltration number is higher, indicating less water can infiltrate into the inside of the ground and a higher discharge rate. Higher in penetration rates can indicate a greater likelihood of landslides (Das and Mukherjee 2005; Elewa et al. 2016; Prabhakaran and Raj 2018)
Junction frequency (Jf)	The score of 1 has the highest impact for landslides, and the scores continue to decline until they reach 0, which has the least impact for landslides	Smaller values imply nearly flat heterogeneity which indicate low risk of landslide, whereas higher values suggest maximum slope heterogeneity which indicate high landslide risk (Das and Lepcha 2019)
Length overland flow (Lg)	The score of 1 has the highest impact for landslides, and the scores continue to decline until they reach 0, which has the least impact for landslides	Higher value implies the greater surface run off which indicate higher chances of landslide occurrences and vice versa (Sonker et al. 2023)
Roughness index (Rn)	The score of 1 has the highest impact for landslides, and the scores continue to decline until they reach 0, which has the least impact for landslides	The roughness value is going to be high after the gradient becomes moderate to steep. If the gradient is steep, it means that landslides are more likely to happen, and vice versa (Strahler 1956; Soni 2017; Rózycka et al. 2017)
Hydrological parameters		
SPI	The score of 1 has the highest impact for landslides, and the scores continue to decline until they reach 0, which has the least impact for landslides	A higher SPI score means that there is more erosion, which shows the steep slope, straight, eroded areas and bedrock (Moore et al. 1991; Moazzam et al. 2020). This indicates higher chances of landslides occurring

Table 4 (continued)

Factor	Scale/weight procedure	Logic for scaling/weight
STI	The score of 1 has the highest impact for landslides, and the scores continue to decline until they reach 0, which has the least impact for landslides	A higher STI score means that sediment can be removed more easily, which means that landslides are more likely to happen (Kalantar et al. 2018; Basu and Pal 2020)
TWI	The score of 1 has the highest impact for landslides, and the scores continue to decline until they reach 0, which has the least impact for landslides	The higher the TWI score, the higher the chances of landslide occurrences because higher TWI indicate higher degree of accumulation of moisture in an area
Rainfall (Rf)	The score of 1 has the highest impact for landslides, and the scores continue to decline until they reach 0, which has the least impact for landslides	Higher rainfall values indicate higher chances of landslides occurring, and vice versa (Basu and Pal 2020; Moazzam et al. 2020)

Table 5 Calculations of the FR and FRn values for different factor classes for landslide susceptibility zonation mapping in the Sikkim Himalaya

Factors	Classes	Classes of the factor/ thematic layers	Number of landslides in classes	Percentage of landslides in classes	Pixels in classes	Percentage of Pixels area in classes	Fr	Frn
Relief parameters								
Absolute relief (Ar)	1.00	< 1119	140.00	29.23	690,330.00	8.18	3.57	0.93
	2.00	1119–1777	226.00	47.18	1,036,978.00	12.29	3.84	1.00
	3.00	1777–2436	71.00	14.82	948,415.00	11.24	1.32	0.34
	4.00	2436–3156	18.00	3.76	936,212.00	11.09	0.34	0.09
	5.00	3156–3815	18.00	3.76	809,573.00	9.59	0.39	0.10
	6.00	3815–4410	6.00	1.25	958,066.00	11.35	0.11	0.03
	7.00	4410–4912	0.00	0.00	1,053,588.00	12.48	0.00	0.00
	8.00	4912–5382	0.00	0.00	1,222,479.00	14.49	0.00	0.00
	9.00	5382–6008	0.00	0.00	631,629.00	7.48	0.00	0.00
	10.00	> 6008	0.00	0.00	152,152.00	1.80	0.00	0.00
Relative relief (Rr)	1.00	< 320	0.00	0.00	93,646.00	1.18	0.00	0.00
	2.00	330–480	0.00	0.00	133,779.00	1.69	0.00	0.00
	3.00	480–640	32.00	6.68	718,194.00	9.07	0.74	0.44
	4.00	640–800	72.00	15.03	1,199,439.00	15.15	0.99	0.60
	5.00	800–960	211.00	44.05	2,096,814.00	26.49	1.66	1.00
	6.00	960–1100	129.00	26.93	1,930,116.00	24.38	1.10	0.66
	7.00	1100–1300	21.00	4.38	924,223.00	11.68	0.38	0.23
	8.00	1300–1400	14.00	2.92	674,424.00	8.52	0.34	0.21
	9.00	1400–1500	0.00	0.00	113,878.00	1.44	0.00	0.00
	10.00	> 1500	0.00	0.00	30,958.00	0.39	0.00	0.00

Table 5 (continued)

Factors	Classes	Classes of the factor/ thematic layers	Number of landslides in classes	Percentage of landslides in classes	Pixels in classes	Percentage of Pixels area in classes	Fr	Frn
Relief ratio (Rh)	1.00	< 0.0033	0.00	0.00	105,148.00	1.33	0.00	0.00
	2.00	0.0033–0.0047	0.00	0.00	164,186.00	2.07	0.00	0.00
	3.00	0.0047–0.0060	27.00	5.64	728,791.00	9.21	0.61	0.37
	4.00	0.0060–0.0074	112.00	23.38	1,283,023.00	16.21	1.44	0.88
	5.00	0.0074–0.0088	222.00	46.35	2,231,622.00	28.19	1.64	1.00
	6.00	0.0088–0.0101	82.00	17.12	1,780,601.00	22.50	0.76	0.46
	7.00	0.0101–0.0115	26.00	5.43	866,656.00	10.95	0.50	0.30
	8.00	0.0115–0.0129	10.00	2.09	612,633.00	7.74	0.27	0.16
	9.00	0.0129–0.0143	0.00	0.00	114,031.00	1.44	0.00	0.00
	10.00	> 0.0143	0.00	0.00	28,780.00	0.36	0.00	0.00
Dissection index (Di)	1.00	< 0.12	1.00	0.21	963,116.00	12.48	0.02	0.00
	2.00	0.12–0.19	8.00	1.67	1,499,227.00	19.43	0.09	0.02
	3.00	0.19–0.25	13.00	2.71	1,214,486.00	15.74	0.17	0.03
	4.00	0.25–0.32	15.00	3.13	1,027,280.00	13.31	0.24	0.05
	5.00	0.32–0.39	48.00	10.02	1,026,122.00	13.30	0.75	0.15
	6.00	0.39–0.46	115.00	24.01	796,176.00	10.32	2.33	0.45
	7.00	0.46–0.53	97.00	20.25	542,692.00	7.03	2.88	0.56
	8.00	0.53–0.61	61.00	12.73	389,472.00	5.05	2.52	0.49
	9.00	0.61–0.68	58.00	12.11	258,744.00	3.35	3.61	0.71
	10.00	> 0.68	63.00	13.15	198,156.00	2.57	5.12	1.00

Table 5 (continued)

Factors	Classes	Classes of the factor/ thematic layers	Number of landslides in classes	Percentage of landslides in classes	Pixels in classes	Percentage of Pixels area in classes	Fr	Frn
Hypsometric integral (HI)	1.00	< 0.32	0.00	0.00	7587.00	0.10	0.00	0.00
	2.00	0.32–0.35	0.00	0.00	39,855.00	0.50	0.00	0.00
	3.00	0.35–0.38	3.00	0.63	193,384.00	2.44	0.26	0.18
	4.00	0.38–0.41	11.00	2.30	436,126.00	5.51	0.42	0.28
	5.00	0.41–0.44	20.00	4.18	697,634.00	8.81	0.47	0.32
	6.00	0.44–0.47	132.00	27.56	1,489,639.00	18.82	1.46	1.00
	7.00	0.47–0.50	133.00	27.77	2,103,112.00	26.57	1.05	0.71
	8.00	0.50–0.53	117.00	24.43	1,993,784.00	25.19	0.97	0.66
	9.00	0.53–0.56	57.00	11.90	854,411.00	10.79	1.10	0.75
	10.00	< 0.56	6.00	1.25	99,939.00	1.26	0.99	0.68
Slope index (Sl)	1.00	< 10	7.00	1.46	735,918.00	9.31	0.16	0.10
	2.00	10–17	38.00	7.93	1,120,068.00	14.17	0.56	0.37
	3.00	17–23	44.00	9.19	1,269,595.00	16.06	0.57	0.37
	4.00	23–28	111.00	23.17	1,336,968.00	16.92	1.37	0.89
	5.00	28–33	114.00	23.80	1,227,301.00	15.53	1.53	1.00
	6.00	33–38	80.00	16.70	965,806.00	12.22	1.37	0.89
	7.00	38–43	53.00	11.06	649,262.00	8.21	1.35	0.88
	8.00	43–49	24.00	5.01	371,711.00	4.70	1.07	0.70
	9.00	49–57	6.00	1.25	181,652.00	2.30	0.55	0.36
	10.00	> 57	2.00	0.42	45,713.00	0.58	0.72	0.47

Table 5 (continued)

Factors	Classes	Classes of the factor/ thematic layers	Number of landslides in classes	Percentage of landslides in classes	Pixels in classes	Percentage of Pixels area in classes	Fr	Frn
Drainage parameters								
Drainage density	1.00	< 1.28	50.00	10.44	664,788.00	8.40	1.24	0.54
	2.00	1.28–1.50	73.00	15.24	1,303,367.00	16.47	0.93	0.40
	3.00	1.50–1.70	88.00	18.37	1,572,093.00	19.86	0.93	0.40
	4.00	1.70–1.88	85.00	17.75	1,445,878.00	18.27	0.97	0.42
	5.00	1.88–2.06	83.00	17.33	1,152,840.00	14.56	1.19	0.51
	6.00	2.06–2.25	49.00	10.23	829,719.00	10.48	0.98	0.42
	7.00	2.25–2.46	23.00	4.80	517,193.00	6.53	0.73	0.32
	8.00	2.46–2.72	10.00	2.09	284,773.00	3.60	0.58	0.25
	9.00	2.72–3.14	17.00	3.55	121,120.00	1.53	2.32	1.00
	10.00	> 3.14	1.00	0.21	23,700.00	0.30	0.70	0.30
Drainage frequency	1.00	< 1.43	0.00	0.00	88,176.00	1.11	0.00	0.00
	2.00	1.43–2.63	13.00	2.71	264,899.00	3.35	0.81	0.54
	3.00	2.63–3.38	47.00	9.81	951,656.00	12.02	0.82	0.54
	4.00	3.38–3.94	93.00	19.42	1,500,077.00	18.95	1.02	0.68
	5.00	3.94–4.43	84.00	17.54	1,625,069.00	20.53	0.85	0.56
	6.00	4.43–4.92	88.00	18.37	1,472,680.00	18.61	0.99	0.65
	7.00	4.92–5.44	81.00	16.91	1,053,705.00	13.31	1.27	0.84
	8.00	5.44–6.04	41.00	8.56	601,426.00	7.60	1.13	0.74
	9.00	6.04–6.87	26.00	5.43	283,680.00	3.58	1.51	1.00
	10.00	> 6.87	6.00	1.25	73,248.00	0.93	1.35	0.89

Table 5 (continued)

Factors	Classes	Classes of the factor/ thematic layers	Number of landslides in classes	Percentage of landslides in classes	Pixels in classes	Percentage of Pixels area in classes	Fr	Frn
Drainage intensity (DI)	1.00	< 0.67	0.00	0.00	55,272.00	0.70	0.00	0.00
	2.00	0.67–1.40	2.00	0.42	139,780.00	1.77	0.24	0.16
	3.00	1.40–1.85	14.00	2.92	356,081.00	4.50	0.65	0.43
	4.00	1.85–2.13	39.00	8.14	939,750.00	11.88	0.69	0.45
	5.00	2.13–2.33	84.00	17.54	1,478,191.00	18.68	0.94	0.62
	6.00	2.33–2.54	123.00	25.68	1,803,136.00	22.79	1.13	0.74
	7.00	2.54–2.74	99.00	20.67	1,477,075.00	18.67	1.11	0.73
	8.00	2.74–2.99	64.00	13.36	1,012,530.00	12.80	1.04	0.69
	9.00	2.99–3.30	46.00	9.60	501,839.00	6.34	1.51	1.00
	10.00	> 3.31	8.00	1.67	148,268.00	1.87	0.89	0.59
Drainage texture (Dt)	1.00	< 0.32	0.00	0.00	85,086.00	1.07	0.00	0.00
	2.00	0.32–0.59	13.00	2.71	264,925.00	3.35	0.81	0.55
	3.00	0.59–0.75	47.00	9.81	942,410.00	11.91	0.82	0.55
	4.00	0.75–0.88	95.00	19.83	1,486,922.00	18.79	1.06	0.71
	5.00	0.88–0.99	82.00	17.12	1,622,848.00	20.50	0.83	0.56
	6.00	0.99–1.10	85.00	17.75	1,476,856.00	18.66	0.95	0.64
	7.00	1.10–1.21	83.00	17.33	1,062,331.00	13.42	1.29	0.87
	8.00	1.21–1.35	42.00	8.77	610,475.00	7.71	1.14	0.76
	9.00	1.35–1.53	26.00	5.43	288,835.00	3.65	1.49	1.00
	10.00	> 1.53	6.00	1.25	74,783.00	0.94	1.33	0.89

Table 5 (continued)

Factors	Classes	Classes of the factor/ thematic layers	Number of landslides in classes	Percentage of landslides in classes	Pixels in classes	Percentage of Pixels area in classes	Fr	Frn
Infiltration number (If)	1.00	<4.31	53.00	11.06	907,430.00	11.47	0.96	0.29
	2.00	4.31–6.32	102.00	21.29	1,917,869.00	24.24	0.88	0.27
	3.00	6.32–8.04	108.00	22.55	1,765,728.00	22.32	1.01	0.31
	4.00	8.04–9.77	85.00	17.75	1,354,578.00	17.12	1.04	0.32
	5.00	9.77–11.64	57.00	11.90	907,759.00	11.47	1.04	0.32
	6.00	11.64–13.65	41.00	8.56	540,907.00	6.84	1.25	0.38
	7.00	13.65–15.95	10.00	2.09	288,644.00	3.65	0.57	0.17
	8.00	15.95–18.96	11.00	2.30	151,389.00	1.91	1.20	0.37
	9.00	18.96–23.42	12.00	2.51	60,294.00	0.76	3.29	1.00
	10.00	>23.42	0.00	0.00	17,324.00	0.22	0.00	0.00
Junction frequency (Jf)	1.00	<3.07	0.00	0.00	133,590.00	1.69	0.00	0.00
	2.00	3.07–3.58	17.00	3.55	428,766.00	5.42	0.66	0.37
	3.00	3.58–4.00	35.00	7.31	811,394.00	10.25	0.71	0.40
	4.00	4.00–4.48	81.00	16.91	1,527,084.00	19.29	0.88	0.49
	5.00	4.48–4.90	92.00	19.21	1,618,231.00	20.44	0.94	0.52
	6.00	4.90–5.40	122.00	25.47	1,573,070.00	19.87	1.28	0.72
	7.00	5.40–5.91	75.00	15.66	1,025,482.00	12.96	1.21	0.67
	8.00	5.91–6.42	34.00	7.10	523,048.00	6.61	1.07	0.60
	9.00	6.42–7.06	17.00	3.55	219,466.00	2.77	1.28	0.71
	10.00	>7.06	6.00	1.25	55,340.00	0.70	1.79	1.00

Table 5 (continued)

Factors	Classes	Classes of the factor/ thematic layers	Number of landslides in classes	Percentage of landslides in classes	Pixels in classes	Percentage of Pixels area in classes	Fr	Frn
Length of overland flow (Lg)	1.00	< 0.64	50.00	10.44	664,788.00	8.40	1.24	0.54
	2.00	0.64–0.75	73.00	15.24	1,303,367.00	16.47	0.93	0.40
	3.00	0.75–0.85	88.00	18.37	1,572,093.00	19.86	0.93	0.40
	4.00	0.85- 0.94	85.00	17.75	1,445,878.00	18.27	0.97	0.42
	5.00	0.94–1.03	83.00	17.33	1,152,840.00	14.56	1.19	0.51
	6.00	1.03–1.12	49.00	10.23	829,719.00	10.48	0.98	0.42
	7.00	1.12–1.23	23.00	4.80	517,193.00	6.53	0.73	0.32
	8.00	1.23–1.36	10.00	2.09	284,773.00	3.60	0.58	0.25
	9.00	1.36–1.57	17.00	3.55	121,120.00	1.53	2.32	1.00
	10.00	> 1.57	1.00	0.21	23,700.00	0.30	0.70	0.30
Ruggedness index (Rn)	1.00	< 0.2597	5.00	1.04	77,011.00	0.96	1.08	0.75
	2.00	0.2597–0.3443	27.00	5.64	310,147.00	3.88	1.45	1.00
	3.00	0.3443–0.4022	50.00	10.44	644,006.00	8.06	1.30	0.89
	4.00	0.4022–0.4481	63.00	13.15	1,109,023.00	13.88	0.95	0.65
	5.00	0.4481–0.4865	97.00	20.25	1,479,429.00	18.51	1.09	0.75
	6.00	0.4865–0.5250	119.00	24.84	1,662,283.00	20.80	1.19	0.82
	7.00	0.5250–0.5634	73.00	15.24	1,291,232.00	16.16	0.94	0.65
	8.00	0.5634–0.6096	34.00	7.10	857,076.00	10.72	0.66	0.46
	9.00	0.6096–0.6673	11.00	2.30	422,989.00	5.29	0.43	0.30
	10.00	> 0.6673	0.00	0.00	139,232.00	1.74	0.00	0.00

Table 5 (continued)

Factors	Classes	Classes of the factor/ thematic layers	Number of landslides in classes	Percentage of landslides in classes	Pixels in classes	Percentage of Pixels area in classes	Fr	Frn
Hydrological parameters								
SPI	1.00	< 1.04	1.00	0.21	162,362.00	2.05	0.10	0.06
	2.00	1.04–2.29	20.00	4.18	817,671.00	10.33	0.40	0.24
	3.00	2.29–3.15	105.00	21.92	1,655,952.00	20.92	1.05	0.63
	4.00	3.15- 3.94	97.00	20.25	1,539,481.00	19.45	1.04	0.62
	5.00	3.94- 4.80	99.00	20.67	1,447,385.00	18.29	1.13	0.68
	6.00	4.80–5.65	75.00	15.66	968,640.00	12.24	1.28	0.77
	7.00	5.65–6.58	36.00	7.52	638,271.00	8.06	0.93	0.56
	8.00	6.58–7.63	20.00	4.18	393,843.00	4.98	0.84	0.50
	9.00	7.63–8.88	21.00	4.38	208,101.00	2.63	1.67	1.00
	10.00	> 8.88	5.00	1.04	83,597.00	1.06	0.99	0.59
STI	1.00	< 1.61	254.00	53.03	4,852,481.00	61.31	0.86	0.41
	2.00	1.61–8.04	187.00	39.04	2,591,070.00	32.73	1.19	0.56
	3.00	8.04–17.68	23.00	4.80	332,901.00	4.21	1.14	0.54
	4.00	17.68–28.94	11.00	2.30	85,386.00	1.08	2.13	1.00
	5.00	28.94–43.40	3.00	0.63	32,889.00	0.42	1.51	0.71
	6.00	43.40–61.09	1.00	0.21	12,777.00	0.16	1.29	0.61
	7.00	61.09–85.20	0.00	0.00	5138.00	0.06	0.00	0.00
	8.00	85.20–120.57	0.00	0.00	1977.00	0.02	0.00	0.00
	9.00	120.57–181.65	0.00	0.00	567.00	0.01	0.00	0.00
	10.00	> 181.65	0.00	0.00	117.00	0.00	0.00	0.00

Table 5 (continued)

Factors	Classes	Classes of the factor/ thematic layers	Number of landslides in classes	Percentage of landslides in classes	Pixels in classes	Percentage of Pixels area in classes	Fr	Frn
TWI	1.00	<4.23	102.00	21.29	1,358,160.00	17.16	1.24	1.00
	2.00	4.23–5.00	119.00	24.84	1,877,750.00	23.72	1.05	0.84
	3.00	5.00–5.76	89.00	18.58	1,571,068.00	19.85	0.94	0.75
	4.00	5.76–6.59	67.00	13.99	1,150,822.00	14.54	0.96	0.78
	5.00	6.59–7.57	48.00	10.02	827,797.00	10.46	0.96	0.77
	6.00	7.57–8.61	19.00	3.97	524,924.00	6.63	0.60	0.48
	7.00	8.61–9.72	19.00	3.97	305,282.00	3.86	1.03	0.83
	8.00	9.72–11.04	11.00	2.30	181,887.00	2.30	1.00	0.81
	9.00	11.04–12.77	5.00	1.04	87,824.00	1.11	0.94	0.76
	10.00	>12.77	0.00	0.00	29,789.00	0.38	0.00	0.00
Rainfall (Rf) (mm/year)	1.00	<2473	95.00	19.96	530,349.00	6.72	2.97	1.00
	2.00	2473–2576	68.00	14.29	3,525,666.00	44.70	0.32	0.11
	3.00	2576–2685	54.00	11.34	1,698,235.00	21.53	0.53	0.18
	4.00	2685–2819	90.00	18.91	582,411.00	7.38	2.56	0.86
	5.00	2819–2959	59.00	12.39	548,152.00	6.95	1.78	0.60
	6.00	2959–3088	64.00	13.45	410,369.00	5.20	2.58	0.87
	7.00	3088–3223	19.00	3.99	147,493.00	1.87	2.13	0.72
	8.00	3223–3363	12.00	2.52	184,544.00	2.34	1.08	0.36
	9.00	3363–3492	5.00	1.05	129,577.00	1.64	0.64	0.22
	10.00	>3492	10.00	2.10	130,461.00	1.65	1.27	0.43

Fig. 3 **a** Figure of the FR values of different relief factor with class of the factors, **b** figure of the FR values of different drainage factor vrs class of the factors **c** figure of the FR values of different hydrological factor vrs class of the factors

relief parameters (Fig. 2), landslide susceptibility zones vary from different relief classes. Low class (1 to 3) of the absolute index (Fig. 2a), the FR value greater than 1 is most effective (very high to high zones, FRn values vary from 0.6 to 1), but FR values less than 1 (in the high absolute index class) are least affective (moderate to low zones, FRn values varies from 0 to 0.6) for the landslide susceptibility, as shown in Fig. 3a and Table 5. Landslides are most common in low-absolute-index (low-altitude) areas. This region is mostly found along the drainage valleys (Teesta and Rangit Rivers) and moderate hill areas of Sikkim's southern region (West, South, and East Sikkim), as shown in Fig. 1. This factor is most responsible for landslide occurrence in the study region. The relative relief and relief ratio (Fig. 2b, c) is very high from classes 4 to 6, indicating moderate relief in Sikkim's southern region, but the graph shows the same variation in FR values, shown in Fig. 3a. The FR values of these classes are greater than 1, which indicates higher chance of the landslide's occurrence because that indicates the effects of erosion or uplift and also indicates the tectonics of the area. FRn values of these classes vary from 0.6 to 1, which is a higher correlation for very high to high susceptibility for landslide occurrences. Classes 1, 2, 3, 7, 8, 9, and 10 of the factors occur in the moderate to low region of the susceptibility for landslides because the FR values are less than 1 and the FRn values lie from 0 to 0.6 (Table 5). This region is shown in the northern region of the study area, which has shown moderate-to-low chances of landslides occurrence. The dissection index (Fig. 2d) of the area is very high, as are the valleys of the region, particularly the Teesta and Rangit River basins, where FR values are greater than 1, indicating the possibility of landslides due to slope degradation or separation degree of landscape changes, as shown in Fig. 3a and Table 5. The FRn of the dissection class such as classes 9 and 10 varies from 0.6 to 1, which indicates a very high to high susceptibility for landslides. The classes 1, 2, 3, 4, 5, 6, 7 and 8 of the dissection occurred in the moderate to low susceptibility region for landslides because the FRn values lie from 0 to 0.6 (Table 5). The hypsometric integral (Fig. 2e) of the area is very high along the valley (Teesta and Rangit River) and on moderate terrain in the region where FR values are greater than 1 (Fig. 3a and Table 5) because it generates a significant amount of surface runoff, which caused sediment erosion and also indicates the tectonic evolution of the region. The tectonic evolution of the rocks indicates a decrease in rigidity, which causes landslides. The FRn value for the classes of the hypsometric integral, such as classes 6 and 10, varies from 0.6 to 1, which indicates a very high to high susceptibility for landslides, and the FRn value for the classes 1–5 of the hypsometric integral varies from 0 to 0.6, which indicates a moderate to low susceptibility. The slope (Fig. 2f) of the area is varying from 0 to 84 degrees, in which the moderate to high gradient is more prone to landslides occurrences where the FR values are greater than 1, as shown in Fig. 3a and Table 5. The very high to high susceptibility zones occur in class 4 to 8 of the slope gradient where the FRn values from 0.6 to 1 and the FRn value for class 1, 2, 3, 9, and 10 of the slopes varies from 0 to 0.6 (Table 5), which indicates a moderate to low susceptibility. The drainage density (Fig. 2g) of the area ranges from 0.71 to 4.24 km/km^2, and drainage density classes 1, 5, and 9 are more vulnerable to landslides due to FR values larger than 1. As indicated in Fig. 3b and Table 5, the very high, high, and moderate susceptibility zones occur in this class 1,4, 5, 6, and 9 of drainage density where the FRn is more than 0.4 and FRn value less than 0.4 indicating low to very low susceptibility of

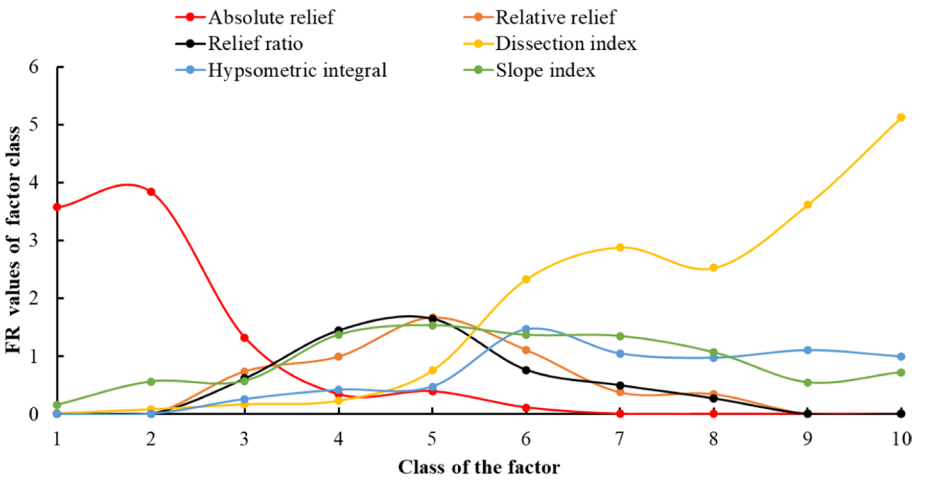
Absolute relief
Relative relief
Relief ratio
Dissection index
Hypsometric integral
Slope index
FR values of factor class
Class of the factor

(a)

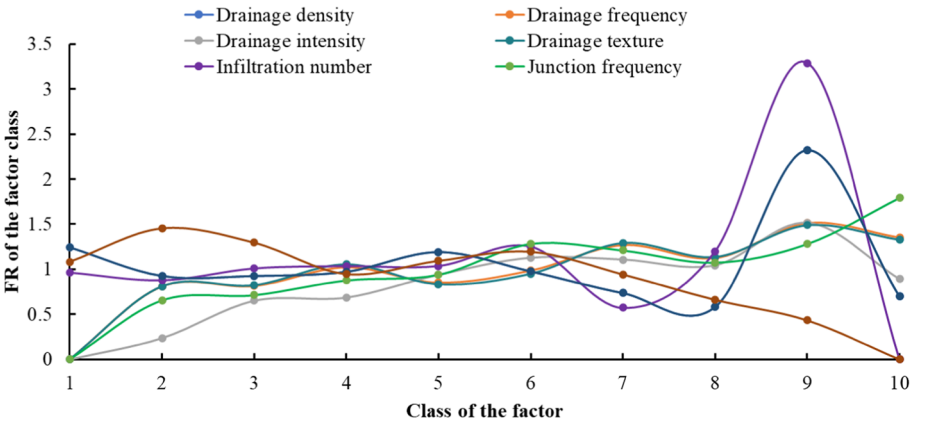
Drainage density
Drainage frequency
Drainage intensity
Drainage texture
Infiltration number
Junction frequency
FR of the factor class
Class of the factor

(b)

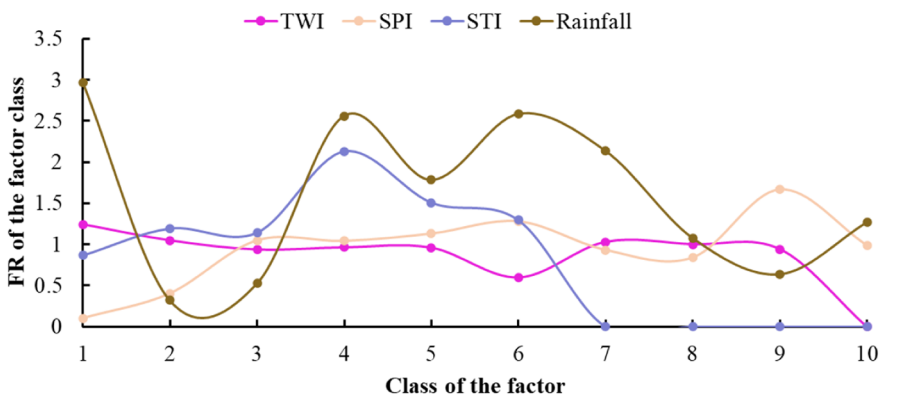
TWI
SPI
STI
Rainfall
FR of the factor class
Class of the factor

(c)

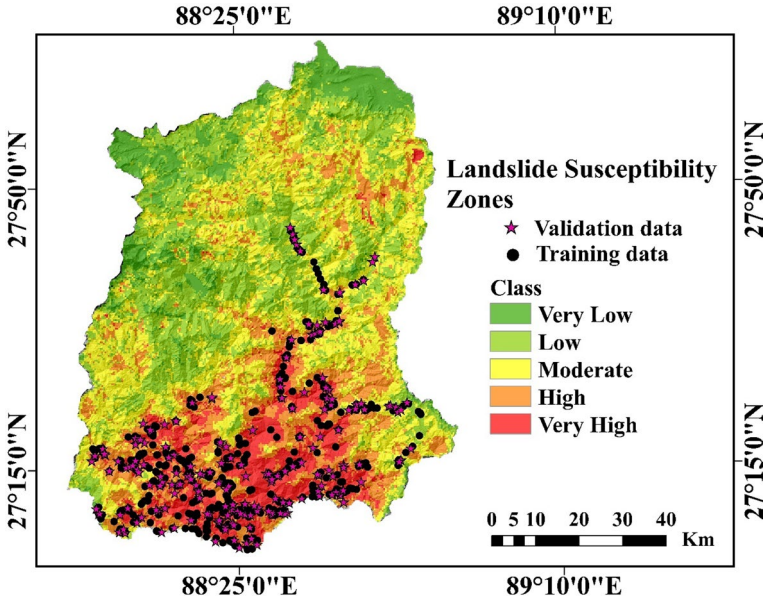

Fig. 4 Landslide Susceptibility map of Sikkim Himalaya

landslide occurrence. The drainage frequency (Fig. 2h) of the area ranges from 0 to 9.57 (number of drainages/km^2), and the drainage frequency of classes 4, 7, 8, 9, and 10 are more susceptible to landslides due to FR values greater than 1. The very high, high, moderate susceptibility zones occur in the class from 2 to 10 of the drainage frequency where the FRn is more than 0.4, this mainly occurs along the valley slope of the southern region of the drainages in the area. FRn value of class 1 is less than 0.4 indicating low to very low susceptibility to landslide occurrence mostly occurs in the northern region of the area as shown in Fig. 3b and Table 5. The drainage intensity (Fig. 2i) of the region ranges from 0 to 4.76, and classes 6, 7, 8, and 9 are more prone to landslides due to FR values greater than 1. The very high, high, and moderate susceptibility zones occur in the class from 6 to 10 of the drainage intensity where FRn is more than 0.4. The drainage texture (Fig. 2j) of the region ranges from 0 to 2.13 (No. of drainages/km), and classes 4, 7, 8, and 9 are more prone to landslides due to FR values greater than 1 (Fig. 3b and Table 5). The very high, high, and moderate susceptibility zones occur in the class from 2 to 10 of the drainage texture where FRn is more than 0.4 and the class 1 of the drainage texture is very low to low susceptibility zones because the FRn value is less than 0.4 (Table 5). The drainage texture and frequency of the region show the same FRn value shown in the graph (Fig. 3b). Infiltration number (Fig. 2k) of the area varies from 0 to 37, and classes 3, 4, 5, 6, 8, and 9 are more prone to landslides due to FR values greater than 1 (Fig. 3b, Table 5). Class 9 of the infiltration number is higher infiltration numbers indicating lower infiltration and higher run-off, which lead to higher occurrences of landslides. The junction frequency (Fig. 2l) of the area varies from 0 to 9, and classes 6 to 10 are more prone to landslides due to FR values greater than 1 (Fig. 3b, Table 5). The very high, high, and moderate susceptibility zones occur in the class from 4 to 10 of the junction frequency where FRn is more than 0.4 and the class 1 to 3 of the junction frequency is very low to low susceptibility zones because FRn value is less than 0.4 (Table 5). Length overland flow (Fig. 2m) varies

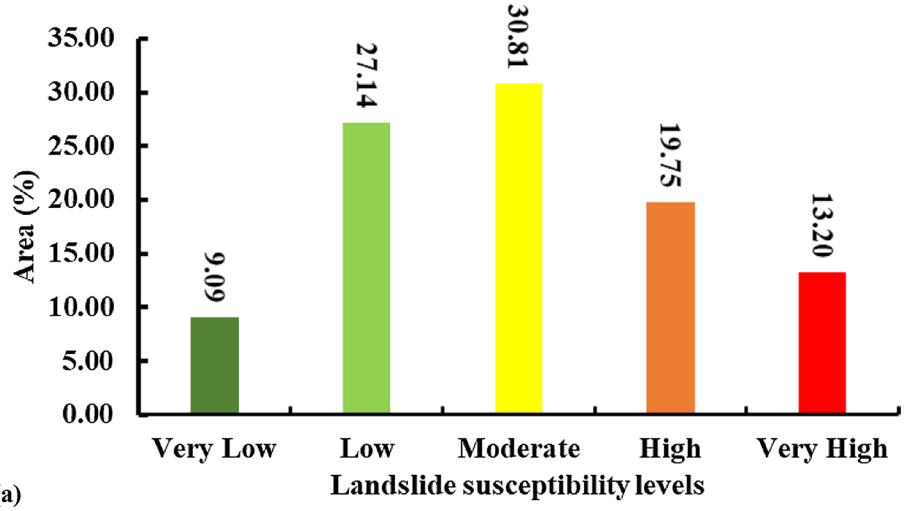

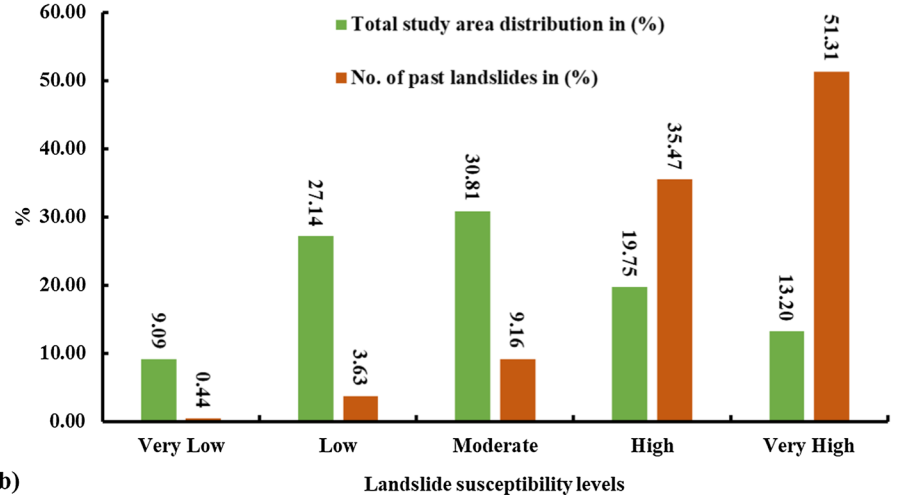

Fig. 5 **a** Landslide susceptibility zones in area (%) of the Sikkim Himalaya, **b** Landslide susceptibility zones in area (%) with respect to number of past landslides in (%) of the Sikkim Himalaya

from 0 to 2.12, and very high, high, and moderate susceptibility zones occur in classes 1, 4, 5, 6, and 9 because FRn values are greater than 0.4. Roughness index (Fig. 2n) varies from 0.0098 to 0.9902, and very high, high, and moderate susceptibility zones occur in classes 1 to 8 because FRn values are greater than 0.4 (Table 5). Low to higher roughness area is highly susceptible to landslides in this area which lies on the river valley side of the region. The SPI (Fig. 2o) of the region varies from − 3.51 to 13.30, and classes 3, 4, 5, 6, and 8 are more prone to landslides due to FR values greater than 1 as shown in Fig. 3c and Table 5. Class 3–10 of SPI has zones of very high, high, and moderate susceptibility for the occurrence of the landslide because FRn values are more than 0.4 (Table 5). The SPI of the

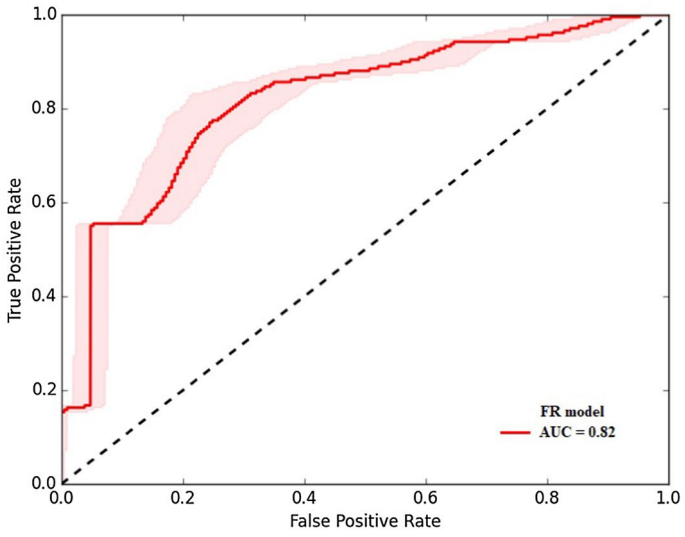

Fig. 6 **a.** The successive rate curve for FR model for LSZ mapping of Sikkim Himalaya, **b.** validation rate curve for FR model for LSZ mapping of Sikkim Himalaya

region increases whenever there is an increasedrisk of landslides occurring in the region. The STI (Fig. 2p) of the region varies from 0 to 409.92 and classes from 2 to 6 are more prone to landslides due to FR values greater than 1 as shown in Fig. 3c and Table 5. Class 1–6 of STI factor has zones of very high to moderate susceptibility for the landslide because FRn values are more than 0.4 (Table 5). The region's TWI (Fig. 2q) ranges from 1.11 to 18.81, and classes 1 through 9 have zones of very high, high, and moderate

sensitivity because FRn values are larger than 0.4 (Table 5). This region has a low to higher TWI, which implies a high susceptibility to landslides. Class of Rainfall 1, 3 to 6 and 10 shows the very high to moderate risk zones of landslide and second most responsible parameter for landslide occurrences as shown in Fig. 2r, 3c and Table 5.

3.2 Importance check of the thematic layers using sensitivity of map removal analysis

The purpose of this method is to explore the consequences of eliminating any of the thematic layers used to estimate the landslide risk zones (LSZ). After deleting each thematic layer, a new LSZ map with the remaining layers overlay is generated. Now, the sensitivity index is estimated using equation () every time.

$$\mathrm{SI} = \frac{\left|\left(\frac{\mathrm{LSZ}}{N}\right) - \left(\frac{\mathrm{LSZ}\prime}{n}\right)\right|}{\mathrm{LSZ}} \times 100$$

where SI represents the sensitivity index linked including an omitted thematic layer, LSZ represents landslide susceptibility zones mapping using each the thematic factors, LSZ′ represents landslide susceptibility zones mapping by eliminating one thematic layer at once, N represents the number of factors utilized in the production of the LSZ map, while n represents the number of factors evaluated in the creation of the LSZ map. The estimated values of all factors, such as Min, Max, Mean and Standard deviation (Table 6). The absolute index and rainfall are the two most sensitive parameters, with standard deviations of 0.44 and 0.42 (Table 6) for thematic layers when mapping landslide susceptibility zones,

Table 6 Statistical analysis of map removal sensitivity analysis for the Landslide susceptibility zonation mapping

Factor Class	Min	Max	Mean	Standard deviation
Absolute index	−3.88	1.82	−0.2	0.44
Relative relief	−3	1.51	0.02	0.32
Relief ratio	−2.94	1.68	0.02	0.33
Dissection index	−2.75	1.44	0.03	0.31
Hypsometric integral	−3.04	1.67	0.08	0.30
Slope index	−2.39	1.65	0.06	0.28
Drainage density	−2.39	1.65	−0.07	0.28
Drainage frequency	−2.39	1.8	0.07	0.28
Drainage intensity	−2.59	1.8	0.07	0.29
Drainage texture	−2.39	1.85	0.08	0.29
Infiltration number	−2.39	1.58	−0.15	0.28
Junction frequency	−3.18	1.34	−0.33	0.28
Length of overland flow	−2.39	1.65	−0.07	0.28
Ruggedness index	−2.59	1.76	0.09	0.28
SPI	−2.69	1.59	0.03	0.28
STI	−2.39	1.65	−0.07	0.28
TWI	−2.59	1.91	0.16	0.28
Rainfall	−4	1.87	−0.05	0.42

respectively. The relative relief, relief ratio, dissection index and hypsometric integral are moderately sensitive parameters because the standard deviations of the thematic layers are 0.32, 0.33, 0.31 and 0.30 (Table 6). However, slope index, drainage density, drainage frequency, drainage intensity, drainage texture, infiltration number, junction frequency, length of overland flow, ruggedness index, SPI, and TWI are showing equal importance according to the standard deviation, shows the almost same value, which varies from 0.28 to 0.29 (Table 6) for the sensitivity analysis for the landslide susceptibility zones mapping.

3.3 Validation of landslide susceptible model using ROC

The validation of the landslide susceptible zones created by the FR model and previous landslide location can be assessed using the receiver operating characteristic (ROC) curve, which is a commonly used statistical tool. The ROC curve was prepared with the use of the Arc SDM tool, which can be add within the Arc GIS software. For this work, the total number of previous landslide locations is 688 and these landslides were randomly divided into two distinct types of data sets: 70% for training data (479 landslides) and 30% for validation data (209 landslides). The area under the curve (AUC) was utilised to execute an analysis of the efficiency of this model (AUC). This curve represents an approximation of the proportion of the method's successive rate as well as its prediction rate. Training and validation data sets are used to execute the model's successive and predication rate. The FR model performs well when the AUC value is closer to 1. The AUC successive rate and validation rate are approximately 82.00% and 84.6%, respectively, as shown in Fig. 6a, b.

4 Conclusion

In this study, morphological and hydrological parameters were considered to generate the landslide susceptibility zonation in Sikkim Himalaya using frequency ratio model and geospatial technologies. The LSZ map has been classified into five different categories such as 'very high (13.20%)', 'high (19.75%)', 'moderate (30.81%)', 'low (27.14%)', and 'very low (9.09%)'. According to this research, the most risky zones for the landslide-prone area are located in the southern region of Sikkim (the South, West, and East Districts of Sikkim). These prone areas of landslides mostly occur in the river valley (mostly in the southern region of the Upper Teesta and Rangit river valleys) and due to deforestation, complex geological and tectonic settings, farming, and other human activities. These most sensitive areas of the relief parameters indicate less than 2500 m of absolute index, classes 5 and 6 (800–960, 960–1100) of relative relief, classes 4 and 5 (0.0060–0.0074, 0.0074–0.0088) of relief ratio, classes 6 to 10 (0.39–0.46, 0.46–0.53, 0.53–0.61, 0.61–0.68, > 0.68) of the dissection index, classes 6, 7, 9 (0.44–0.47, 0.47–0.50, 0.53–0.56) of hypsometric integral, classes 4 to 8 (23–28, 28–33, 33–38, 38–43, 43–49) of slope index in which the FR values greater than 1. However, most sensitive areas of the drainage parameters indicate classes 1, 5, 9 (< 1.28, 1.88–2.06, 2.72–3.14) of drainage density, classes 4,7 to 10 (3.38–3.94, 4.92–5.44, 5.44–6.04, 6.04–6.87, > 6.87) of the drainage frequency, classes 6 to 9 (2.33–2.54, 2.54–2.74, 2.74–2.99, 2.99–3.30) of drainage intensity, classes 4, 7 to 10 (0.75–0.88, 1.10–1.21, 1.21–1.35, 1.35–1.53, > 1.53) of drainage texture, classes 3 to 6 (6.32–8.04, 8.04–9.77, 9.77–11.64, 11.64–13.65) and 8 to 9 (15.95–18.96, 18.96–23.42) of infiltration number, classes 6 to 10 (4.90–5.40, 5.40–5.91, 5.91–6.42, 6.42–7.06, > 7.06) of junction frequency, classes 1, 5, 9 (< 0.64, 0.94–1.03, 1.36–1.57) of

the length of overland flow, and classes 1 to 3 (< 0.2597, 0.2597–0.3443, 0.3443–0.402) and 5 to 6 (0.4481–0.4865, 0.4865–0.5250) in which classes the FR values is greater than 1. Other most sensitive areas of the drainage parameters indicate classes 3 to 6 (2.29–3.15, 3.15- 3.94, 3.94- 4.80, 4.80–5.65) and 9 (7.63–8.88) of SPI, classes of 2 to 6 (1.61–8.04, 8.04–17.68, 17.68–28.94, 28.94–43.40, 43.40–61.09) of STI, classes 1, 2, 7, 8 (< 4.23, 4.23–5.00, 8.61–9.72, 9.72–11.04) of TWI, and classes 1 (< 2473), 4 to 8 (2685–2819, 2819–2959, 2959–3088, 3088–3223, 3223–3363), 10 (> 3492) of rainfall in which the FR values is higher than 1. Single thematic layer removal analysis is used for thematic layer sensitivity for landslide susceptibility zonation mapping. The absolute index and rainfall are highly influential factors for landslides. This finding is validated by using the ROC curve, which provides an accuracy assessment of around 84.6% for the model. The future scope of the landslide susceptibility zonation mapping of this study may indicate advanced predictive modelling and early warning systems, integrating with remote sensing, GIS, and FR model technologies. Additionally, this research may focus on sustainable mitigation strategies and policy frameworks to minimize the impact of landslides in vulnerable regions, fostering a safer environment for communities in this region.

Acknowledgements The authors express their sincere gratitude to the anonymous reviewer for their invaluable comments, which significantly enhanced the quality and readability of the manuscript. They also appreciate the cooperation and valuable suggestions provided by the editor, whose support was instrumental in improving the work. Additionally, Swarnim and I.S. extend their heartfelt thanks to the University Grants Commission (U.G.C.), New Delhi, for awarding them Junior and Senior Research Fellowships, respectively.

Authorscontributions JNT: Conceptualized the problem, resources and supervision; IS and S: methodology and formal analysis, original draft preparation. IS, S, JNT: writing—discussion, review and editing. All authors have read and agreed to the published version of the manuscript.

Funding Irjesh Sonker and Swarnim thankfully acknowledge University Grants Commission (U.G.C.), New Delhi, for Junior and Senior Research Fellowship awarded to them, respectively.

Data availability Data and material are given in the manuscript.

Declarations

Competing interests This is to declare by all the authors that no financial and personal relationships with other people or organizations have been taken and there is no conflict of interest with other people or organizations.

Ethical responsibilities of authors
Authors declare that they follow the ethical responsibility of the Journal.

References

Abu El-Magd SA, Orabi HO, Ali SA, Parvin F, Pham QB (2021) An integrated approach for evaluating the flash flood risk and potential erosion using the hydrologic indices and morpho-tectonic parameters. Environ Earth Sci 80(20):1–17. https://doi.org/10.1007/s12665-021-10013-0

Adhikari S (2020) Morphometric analysis of a drainage basin: a study of Ghatganga River, Bajhang district, Nepal. Geogr Base 7:127–144. https://doi.org/10.3126/tgb.v7i0.34280

Agarwal CS (1998) Study of drainage pattern through aerial data in Naugarh area of Varanasi district, U.P. J Indian Soc Remote Sens 26:169–175

Ahmad I, Dar MA, Teka AH, Gebre T, Gadissa E, Tolosa AT (2019) Application of hydrological indices for erosion hazard mapping using spatial analyst tool. Environ Monit Assess. https://doi.org/10.1007/s10661-019-7614-x

Anbalagan R, Kumar R, Lakshmanan K, Parida S, Neethu S (2015) Landslide hazard zonation mapping using frequency ratio and fuzzy logic approacha case study of Lachung valley, Sikkim. Geoenviron Disasters 2(1):5. https://doi.org/10.1186/s40677-014-0009-y

Babu KJ, Sreekumar S, Aslam A (2016) Implication of drainage basin parameters of a tropical river basin of South India. Appl Water Sci 6(1):67–75. https://doi.org/10.1007/s13201-014-0212-8

Basu T, Pal S (2019) RS-GIS based morphometrical and geological multi-criteria approach to the landslide susceptibility mapping in Gish River Basin, West Bengal, India. Adv Space Res 63(3):1253–1269. https://doi.org/10.1016/j.asr.2018.10.033

Basu T, Pal S (2020) A GIS—based factor clustering and landslide susceptibility analysis using AHP for Gish River basin, India. Environ Dev Sustain. https://doi.org/10.1007/s10668-019-00406-4

Beven KJ, Kirkby MJ (1979) A physically based, variable contributing area model of basin hydrology/Un modele a base physique de zone d'appel variable de l'hydrologie du bassin versant. Hydrol Sci J 24(1):43–69

Bhasin R, Grimstad E, Larsen JO, Dhawan AK, Singh R, Verma SK, Venkatachalam K (2002) Landslide hazards and mitigation measures at Gangtok, Sikkim Himalaya. Eng Geol 64(4):351–368. https://doi.org/10.1016/S0013-7952(01)00096-5

Bhatt SC, Singh R, Ansari MA, Bhatt S (2020) Quantitative morphometric and morphotectonic analysis of Pahuj catchment basin, central India. J Geol Soc India 96(5):513–520. https://doi.org/10.1007/s12594-020-1590-1

Bhattacharya SK (2012) Landslide disaster perception of the AILA cyclone in the Darjeeling town, West Bengal. India Int J Geomat Geosci 3(1):21–27

Bhattacharya SK (2013) The study of paglajhora landslide in the Darjeeling hills, West Bengal, India. Indian J Spat Sci 40(1):21–27

Binaghi E, Luzi L, Madella P, Pergalani F, Rampini A (1998) Slope instability zonation: a comparison between certainty factor and fuzzy Dempster–Shafer approaches. Nat Hazards 17(1):77–97

Chakrabortty R, Pal SC, Roy P, Saha A, Chowdhuri I (2022) Novel ensemble approach for landslide susceptibility index assessment in a mountainous environment of India. Geocarto Int 37(26):13311–13336. https://doi.org/10.1080/10106049.2022.2076924

Chamling M (2013) Landslides: a geographical review in and around PaglaJhora region of the Eastern Himalayan belt of Darjeeling, West Bengal. Indian J Res 2(8):1–3

Choi J, Oh HJ, Lee HJ, Lee C, Lee S (2012) Combining landslide susceptibility maps obtained from frequency ratio, logistic regression, and artificial neural network models using ASTER images and GIS. Eng Geol 124:12–23

Chopra R, Dhiman RD, Sharma PK (2005) Morphometric analysis of sub-watersheds in Gurdaspur district, Punjab using remote sensing and GIS techniques. J Indian Soc Remote Sens 33(4):531–539. https://doi.org/10.1007/BF02990738

Chowdhuri I, Pal SC, Janizadeh S, Saha A, Ahmadi K, Chakrabortty R, Islam ARMT, Roy P, Shit M (2022a) Application of novel deep boosting framework-based earthquake induced landslide hazards prediction approach in Sikkim Himalaya. Geocarto Int 37(26):12509–12535. https://doi.org/10.1080/10106049.2022.2068675

Chowdhuri I, Pal SC, Saha A, Roy P, Chakrabortty R, Shit M (2022b) Application of novel framework approach for assessing rainfall induced future landslide hazard to world heritage sites in Indo-Nepal-Bhutan Himalayan region. Geocarto Int 37(27):17742–17776. https://doi.org/10.1080/10106049.2022.2134464

Claessens L, Temme AJAM, Schoorl JM (2013) Mass-movement causes: changes in slope angle. Treatise Geomorphol. https://doi.org/10.1016/B978-0-12-374739-6.00167-6

Clarke JI (1996) Morphometry from maps. In: Essays in geomorphology. Elsevier Publication. Co., New York, pp 235–274

Cox RT (1994) Analysis of drainage-basin symmetry as a rapid technique to identify areas of possible Quaternary tilt-block tectonics: an example from the Mississippi Embayment. Geol Soc Am Bull 106(5):571–581. https://doi.org/10.1130/0016-7606(1994)106%3c0571:AODBSA%3e2.3.CO;2

Dai FC, Lee CF, Li J, Xu ZW (2001) Assessment of landslide susceptibility on the natural terrain of Lantau Island, Hong Kong. Environ Geol 40(3):381–391

Das G, Lepcha K (2019) Application of logistic regression (LR) and frequency ratio (FR) models for landslide susceptibility mapping in Relli Khola river basin of Darjeeling Himalaya, India. SN Appl Sci. https://doi.org/10.1007/s42452-019-1499-8

Das AK, Mukherjee S (2005) Drainage morphometry using satellite data and GIS in Raigad district, Maharashtra. J Geol Soc India 65:577–586

Deolia R, Pande A (2014) Spatial distribution of dissection index (erosion intensity) versus geomorphological environment in Parkha Watershed, Central Himalaya. Ind J Geogr Environ 13:11

Devkota KC, Regmi AD, Pourghasemi HR, Yoshida K, Pradhan B, Ryu IC, Dhital MR, Althuwaynee OF (2013) Landslide susceptibility mapping using certainty factor, index of entropy and logistic regression models in GIS and their comparison at Mugling-Narayanghat road section in Nepal Himalaya. Nat Hazards 65(1):135–165. https://doi.org/10.1007/s11069-012-0347-6

Donnarumma A, Revellino P, Grelle G, Guadagno FM (2013) Landslide science and practice. Landslide Sci Pract 1:425–433. https://doi.org/10.1007/978-3-642-31325-7

Dou J, Yamagishi H, Pourghasemi HR, Yunus AP, Song X, Xu Y, Zhu Z (2015) An integrated artificial neural network model for the landslide susceptibility assessment of Osado Island. Jpn Nat Hazards 78:1749–1776

Elewa HH, Ramadan EM, Nosair AM (2016) Spatial-based hydro-morphometric watershed modeling for the assessment of flooding potentialities. Environ Earth Sci 75(906):927. https://doi.org/10.1007/s12665-016-5692-4

Faniran A (1968) The index of drainage intensity–a provisional new drainage factor. Aust J Sci 31:328–330

Farhan Y (2017) Morphometric Assessment of Wadi Wala Watershed, Southern Jordan using ASTER (DEM) and GIS. J Geogr Inf Syst 09(02):158–190. https://doi.org/10.4236/jgis.2017.92011

Ghosh D (2015) Landslide susceptibility analysis from morphometric parameter analysis of RiyongKhola basin, West Sikkim, India: a geospatial approach. Int J Geol Earth Environ Sci 5(54):65

Gupta RP (2003) Remote sensing geology, 2nd edn. Springer-Verlag, Berlin Heidelberg

Gupta RP, Joshi BC (1990) Landslide hazard zonation using the GIS approach—a case study from the Ramganga catchment, Himalayas. Eng Geol 28:119–131

Gupta N, Pal SK, Das J (2022) GIS-based evolution and comparisons of landslide susceptibility mapping of the East Sikkim Himalaya. Spat Sci 3:359–384. https://doi.org/10.1080/19475683.2022.2040587

Horton RE (1932) Drainage basin characteristics. Am Geophys Union Trans 13:350–361

Horton RE (1945) Erosional development of streams and their drainage basins: hydrophysical approach to quantitative morphology. Geol Soc Am Bull 56:275–370

Ilanloo M (2011) A comparative study of fuzzy logic approach for landslide susceptibility mapping using GIS: an experience of Karaj dam basin in Iran. Procedia Soc Behav Sci 19:668–676. https://doi.org/10.1016/j.sbspro.2011.05.184

Islam ARMT, Saha A, Ghose B, Pal SC, Chowdhuri I, Mallick J (2022) Landslide susceptibility modeling in a complex mountainous region of Sikkim Himalaya using new hybrid data mining approach. Geocarto Int 37(25):9021–9046. https://doi.org/10.1080/10106049.2021.2009920

Kalantar B, Pradhan B, Amir Naghibi S, Motevalli A, Mansor S (2018) Assessment of the effects of training data selection on the landslide susceptibility mapping: a comparison between support vector machine (SVM), logistic regression (LR) and artificial neural networks (ANN). Geomat Nat Haz Risk 9(1):49–69. https://doi.org/10.1080/19475705.2017.1407368

Kale VS, Gupta A (2001) Introduction to geomorphology. Orient Longman Ltd., India, pp 82–101

Kannaujiya S, Chattoraj SL, Jayalath D, Champati ray PK, Bajaj K, Podali S, Bisht MP (2019) Integration of satellite remote sensing and geophysical techniques (electrical resistivity tomography and ground penetrating radar) for landslide characterization at Kunjethi (Kalimath), Garhwal Himalaya, India. Nat Hazards 97(3):1191–1208. https://doi.org/10.1007/s11069-019-03695-0

Kaur H, Gupta S, Parkash S, Thapa R, Gupta A, Khanal GC (2019) Evaluation of landslide susceptibility in a hill city of Sikkim Himalaya with the perspective of hybrid modelling techniques. Spat Sci 25(2):113–132. https://doi.org/10.1080/19475683.2019.1575906

Kayastha P, Dhital MR, Smedt FD (2013) Evaluation and comparison of GIS based landslide susceptibility mapping procedures in Kulekhani watershed Nepal. J Geol Soc India 81(2):219–231. https://doi.org/10.1007/s12594-013-0025-7

Kumar V, Gupta V, Jamir I (2018) Hazard evaluation of progressive Pawari landslide zone, Satluj valley, Himachal Pradesh. India Nat Hazards 93(2):1029–1047. https://doi.org/10.1007/s11069-018-3339-3

Lee S (2005) Application of logistic regression model and its validation for landslide susceptibility mapping using GIS and remote sensing data. Int J Rem Sens 26(7):1477–1491

Lee S (2014) Geological application of geographic information system. Korea Inst Geosci Min Resour 9–15:109–118

Lin LL, Wang CW, Chiu CL, Ko YC (2011) A study of rationality of slopeland use in view of land preservation. Paddy Water Environ 9:257–266

Long NT, De Smedt F (2018) Analysis and mapping of rainfall-induced landslide susceptibility in A luoi district, thua thien hue province. Vietnam Water (switzerland). https://doi.org/10.3390/w11010051

Mahadevaswamy G, Nagaraju D, Siddalingamurthy S, Lakshmamma MSL, Nagesh PC, Rao K (2011) Morphometric analysis of Nanjangud taluk, Mysore district, Karnataka, India, using GIS techniques. Int J Geomat Geosci 1:179–187

Mandal S, Maiti R (2013) Assessing the triggering rainfall-induced landslip events in the Shivkhola Watershed of Darjeeling Himalaya, West Bengal. Eur J Geogr 4(3):21–33
Mandal B, Mandal S (2016) Assessment of mountain slope instability in the Lish River basin of Eastern Darjeeling Himalaya using frequency ratio model (FRM). Model Earth Syst Environ 2(3):1–14. https://doi.org/10.1007/s40808-016-0169-8
Melton MA (1957) An analysis of the relation among elements of climate, surface properties, and geomorphology. Department of Geology, Columbia University, New York
Mersha T, Meten M (2020) GIS-based landslide susceptibility mapping and assessment using bivariate statistical methods in Simada area, Northwestern Ethiopia. Geoenviron Disasters 7:20. https://doi.org/10.1186/s40677-020-00155-x
Mezughi TH, Akhir JM, Rafek AG, Abdullah I (2011) Landslide susceptibility assessment using frequency ratio model applied to an area along the E-W Highway (Gerik-Jeli). Am J Environ Sci 7:43–50
Miller VC (1953) A quantitative geomorphic study of drainage basin characteristics in the Clinch Mountain area, Varginia and Tennessee. J Geol 1:112–113
Mirdda HA, Bera S, Siddiqui MA, Singh B (2020) Analysis of bi-variate statistical and multi-criteria decision-making models in landslide susceptibility mapping in lower Mandakini Valley, India. GeoJournal 85(3):681–701. https://doi.org/10.1007/s10708-019-09991-3
Mishra AK, Rai SC (2020) Geo-hydrological inferences through morphometric aspects of the Himalayan glacial-fed river: a case study of the Madhyamaheshwar River basin. Arab J Geosci 13(13):2. https://doi.org/10.1007/s12517-020-05571-9
Moazzam MFU, Vansarochana A, Boonyanuphap J, Choosumrong S, Rahman G, Djueyep GP (2020) Spatio-statistical comparative approaches for landslide susceptibility modeling: case of Mae Phun, Uttaradit Province, Thailand. SN Appl Sci 2(3):1–15. https://doi.org/10.1007/s42452-020-2106-8
Mohammady M, Pourghasemi HR, Pradhan B (2012) Landslide susceptibility mapping at Golestan Province, Iran: a comparison between frequency ratio, Dempster-Shafer, and weights-of-evidence models. J Asian Earth Sci 61:221–236
Moore ID, Wilson JP (1992) Length-slope factors for the revised universal soil loss equation: simplified method of esti- mation. J Soil Water Conserv 47(5):423–428
Moore ID, Grayson RB, Ladson AR (1991) Digital terrain modelling: a review of hydrological, geomorphological, and biological applications. Hydrol Process 5(1):3–30. https://doi.org/10.1002/hyp.3360050103
Moore ID, Gessler PE, Nielsen GA, Peterson GA (1993) Soil attribute prediction using terrain analysis. Soil Sci Soc Am J 57(2):61. https://doi.org/10.2136/sssaj1993.03615995005700020026x
Mueller JE (1968) An introduction to the hydraulic and topographic sinuosity indexes. Ann Assoc Am Geogr 58:371–385
Nakileza BR, Nedala S (2020) Topographic influence on landslides characteristics and implication for risk management in upper Manafwa catchment, Mt Elgon Uganda. Geoenviron Disasters 7:1–13
Nefeslioglu HA, Duman TY, Durmaz S (2008) Landslide susceptibility mapping for a part of tectonic kelkit valley (eastern black sea region of Turkey). Geomorphology 94:401–418
Nefeslioglu HA, Sezer E, Gokceoglu C, Bozkir AS, Duman TY (2010) Assessment of landslide susceptibility by decision trees in the metropolitan area of Istanbul, Turkey, 2010. Math Probl Eng. https://doi.org/10.1155/2010/901095
Oguchi T (1997) Drainage density and relative relief in humid steep mountains with frequent slope failure. Earth Surf Process Landf 22:107–120
Pal SC, Chowdhuri I (2019) GIS-based spatial prediction of landslide susceptibility using frequency ratio model of Lachung River basin, North Sikkim, India. SN Appl Sci 1(5):1–25. https://doi.org/10.1007/s42452-019-0422-7
Pandey VK, Sharma KK, Bandooni SK (2018) Characteristics of large landslides and application of frequency ratio model for susceptibility assessment, lower Jalal catchment (Himachal Pradesh). Int J Res Geogr 4(1):17–26. https://doi.org/10.20431/2454-8685.0401004
Pawluszek K, Borkowski A (2017) Impact of DEM-derived factors and analytical hierarchy process on landslide susceptibility mapping in the region of Rożnów Lake, Poland. Nat Hazards 86(2):919–952
Pourghasemi HR, Mohammady M, Pradhan B (2012a) Landslide susceptibility mapping using index of entropy and conditional probability models in GIS: Safarood basin, Iran. CATENA 97:71–84
Pourghasemi HR, Pradhan B, Gokceoglu C (2012b) Application of fuzzy logic and analytical hierarchy process (AHP) to landslide susceptibility mapping at Haraz watershed. Iran Nat Hazards 63(2):965–996
Prabhakaran A, Jawahar Raj N (2018) Drainage morphometric analysis for assessing form and processes of the watersheds of Pachamalai hills and its adjoinings, Central Tamil Nadu, India. Appl Water Sci 8(1):1–19. https://doi.org/10.1007/s13201-018-0646-5

Pradhan B, Sezer EA, Gokceoglu C, Buchroithner MF (2010) Landslide susceptibility mapping by neuro-fuzzy approach in a landslide prone area (Cameron Highlands, Malaysia). Geosci Remote Sens IEEE Trans 48(12):4164–4177

Qiu H, Cui P, Regmi AD, Hu S, Zhang Y, He Y (2018) Landslide distribution and size versus relative relief (Shaanxi Province, China). Bull Eng Geol Env 77(4):1331–1342. https://doi.org/10.1007/s10064-017-1121-5

Rai PK, Chandel RS, Mishra VN, Singh P (2018) Hydrological inferences through morphometric analysis of lower Kosi river basin of India for water resource management based on remote sensing data. Appl Water Sci 8(1):1–16. https://doi.org/10.1007/s13201-018-0660-7

Rawat MS (2012) Statistical analysis of Landslide in South district, Sikkim, India: using remote sensing and GIS. IOSR J Environ Sci Toxicol Food Technol 2(3):47–61. https://doi.org/10.9790/2402-0234761

Rawat MS, Dobhal R, Joshi V, Sundriyal Y (2017) Landslide hazard zonation study in Eastern Indian Himalayan Region. Int J Georesources Environ 3(1):35–46. https://doi.org/10.15273/ijge.2017.01.005

Reddy GPO, Maji AK, Gajbhiye KS (2002) GIS for morphometric analysis of drainage basins. GIS India 11(4):9–14

Rekha VB, George AV, Rita M (2011) Morphometric analysis and micro-watershed prioritization of Peruvanthanam sub-watershed, the Manimala River basin, Kerala, South India. Environ Res Eng Manage 3(57):6–14

Rózycka M, Migoń P, Michniewicz A (2017) Topographic wetness index and terrain ruggedness index in geomorphic characterisation of landslide terrains, on examples from the Sudetes, SW Poland. Z Fur Geomorphol 61:61–80. https://doi.org/10.1127/zfg_suppl/2016/0328

Saha A, Pal SC, Santosh M, Janizadeh S, Chowdhuri I, Norouzi A, Roy P, Chakrabortty R (2021) Modelling multi-hazard threats to cultural heritage sites and environmental sustainability: the present and future scenarios. J Clean Prod. https://doi.org/10.1016/j.jclepro.2021.128713

Saha A, Pal SC, Chowdhuri I, Chakrabortty R, Roy P (2022) Understanding the scale effects of topographical variables on landslide susceptibility mapping in Sikkim Himalaya using deep learning approaches. Geocarto Int 37(27):17826–17852. https://doi.org/10.1080/10106049.2022.2136255

Sangchini EK, Emami SN, Tahmasebipour N, Pourghasemi HR, Naghibi SA, Arami SA, Pradhan B (2016) Assessment and comparison of combined bivariate and AHP models with logistic regression for landslide susceptibility mapping in the Chaharmahal-e-Bakhtiari Province, Iran. Arab J Geosci. https://doi.org/10.1007/s12517-015-2258-9

Sarkar S, Kanungo DP, Patra AK, Kumar P (2006) GIS based landslide susceptibility mapping—a case study in Indian Himalaya. Universal Academy Press Inc., Tokyo, pp 617–624

Schumm SA (1956) Evolution of drainage systems and slopes in badlands at Perth Amboy, New Jersey. Geol Soc Am Bull 67:597–646

Skilodimou HD, Bathrellos GD, Koskeridou E, Soukis K, Rozos D (2018) Physical and anthropogenic factors related to landslide activity in the northern Peloponnese, Greece. Land. https://doi.org/10.3390/land7030085

Smith KG (1950) Standards for grading texture of erosional topography. Am J Sci 248:655–668

Soni S (2017) Assessment of morphometric characteristics of Chakrar watershed in Madhya Pradesh India using geospatial technique. Appl Water Sci 7(5):2089–2102. https://doi.org/10.1007/s13201-016-0395-2

Soni SK, Tripathi S, Maurya AK (2013) GIS based morphometric characterization of mini-watershed—Rachhar Nala of Anuppur District Madhya Pradesh. Int J Adv Technol Eng Res 3(3):32–38

Sonker I, Tripathi JN (2022) Remote sensing and GIS-based landslide susceptibility mapping using frequency ratio method in Sikkim Himalaya. Quat Sci Adv 8:100067. https://doi.org/10.1016/j.qsa.2022.100067

Sonker I, Tripathi JN, Singh AK (2021) Landslide susceptibility zonation using geospatial technique and analytical hierarchy process in Sikkim Himalaya. Quat Sci Adv 4:100039. https://doi.org/10.1016/j.qsa.2021.100039

Sonker I, Tripathi JN, Singh AK (2023) Morphomertic and neotectonic study of Upper Teesta River basin, Sikkim Himalaya using geospatial techniques. J Appl Geophys 212:104978. https://doi.org/10.1016/j.jappgeo.2023.104978

Sörensen R, Zinko U, Seibert J (2006) On the calculation of the topographic wetness index: evaluation of different methods based on field observations. Hydrol Earth Syst Sci 10:101–112

Sreedevi PD, Sreekanth PD, Khan HH, Ahmed S (2013) Drainage morphometry and its influence on hydrology in a semi-arid region: using SRTM data and GIS. Environ Earth Sci 70(2):839–848

Strahler AN (1952) Hypsometric (area-altitude) analysis of erosional topography. Geol Soc Am Bull 63:1117–1142

Strahler AN (1956) Quantitative slope, analysis. Bull Geol Soc Am 67:571–596

Strahler AN (1964) Quantitative geomorphology of drainage basins and channel networks. In: Handbook of applied hydrology. McGraw-Hill, New York, pp 439–476
Sur U, Singh P, Meena SR (2020) Landslide susceptibility assessment in a lesser Himalayan road corridor (India) applying fuzzy AHP technique and earth-observation data. Geomat Nat Hazards Risk 11(1):2176–2209. https://doi.org/10.1080/19475705.2020.1836038
Taloor AK, Adimalla N, Goswami A (2021a) Remote sensing and GIS applications in geoscience. Appl Comput Geosci 11:1–3. https://doi.org/10.1016/j.acags.2021.100065
Taloor AK, Joshi MN, Kotlia BS, Alam A, Kothyari GC, Kandregula RS, Singh AK, Dumka RK (2021b) Tectonic imprints of landscape evolution in the Bhilangana and Mandakini basin, Garhwal Himalaya, India: a geospatial approach. Quat Int 575–576:21–36. https://doi.org/10.1016/j.quaint.2020.07.021
Taloor AK, Kothyari G, Goswami A (2021c) Remote sensing and GIS applications in quaternary science. Quat Int 574(575):1–4. https://doi.org/10.1016/j.quaint.2021.02.001
Taloor AK, Kothyari G, Goswami A, Mishra A (2022) Geospatial technology applications in quaternary science. Quat Sci Adv 7:100059. https://doi.org/10.1016/j.qsa.2022.100059
Tripathi JN, Sonker I, Tripathi S, Singh AK (2022) Climate change traces on Lhonak Glacier using geospatial tools. Quat Sci Adv 8:100065. https://doi.org/10.1016/j.qsa.2022.100065
Van Westen CJ (1994) GIS in landslide hazard zonation: a review, with examples from the Andes of Colombia. Taylor & Francis, Basingstoke, pp 135–165
Velayudham J, Kannaujiya S, Sarkar T, Taloor AK, Bisht MP, Chawla S, Pal SK (2021) Comprehensive study on evaluation of Kaliasaur Landslide attributes in Garhwal Himalaya by the execution of geospatial, geotechnical and geophysical methods. Quat Sci Adv 3:100025. https://doi.org/10.1016/j.qsa.2021.100025
Wu Y, Li W, Wang Q, Liu Q, Yang D, Xing M, Pei Y, Yan S (2016) Landslide susceptibility assessmentusing frequency ratio, statistical index and certainty factor models for the Gangu County, China. Arabian J Geosci 9(2):1–16. https://doi.org/10.1007/s12517-015-2112-0
Yalcin A, Reis S, Aydinoglu AC, Yomralioglu T (2011) A GIS-based comparative study of frequency ratio, analytical hierarchy process, bivariate statistics and logistics regression methods for landslide susceptibility mapping in Trabzon, NE Turkey. CATENA 85(3):274–287
Yangchan J, Jain AK, Tiwari AK, Sood A (2015) IJSER 61015-1023 Vinutha D N and Janardhana M R 2014 IJIRSET, pp 5516–524
Yilmaz I (2009) Landslide susceptibility mapping using frequency ratio, logistic regression, artificial neural networks and their comparison: a case study from Kat landslides (Tokat-Turkey). Comput Geosci 35:1125–1138
Zhao C, Lu Z (2018) Remote sensing of landslides-a review. Rem Sens 10(2):8–13